

issn 0065-3713

INSTITUT D'AERONOMIE SPATIALE DE BELGIQUE

3 - Avenue Circulaire

B - 1180 BRUXELLES

AERONOMICA ACTA

A - N° 343 - 1989

Ultraviolet absorption spectrum of trifluoro-bromo-methane,
difluoro-dibromo-methane and difluoro-bromo-chloro-methane
in the vapor phase

by

D. GILLOTAY and P.C. SIMON

BELGISCH INSTITUUT VOOR RUIMTE-AERONOMIE

3 - Ringlaan

B - 1180 BRUSSEL

FOREWORD

This paper is accepted for publication in "Journal of Atmospheric Chemistry".

AVANT-PROPOS

Cet article est accepté pour publication dans le "Journal of Atmospheric Chemistry".

VOORWOORD

Dit werk werd voor publicatie aanvaard in "Journal of Atmospheric Chemistry".

VORWORT

Diese Arbeit wurde akzeptiert für Publikation in "Journal of Atmospheric Chemistry".

ULTRAVIOLET ABSORPTION SPECTRUM OF TRIFLUORO-BROMO-METHANE,
DIFLUORO-DIBROMO-METHANE AND DIFLUORO-BROMO-CHLORO-METHANE
IN THE VAPOR PHASE.

D. Gillotay and P.C. Simon

Institut d'Aronomie Spatiale de Belgique
Avenue Circulaire, 3, B-1180 Bruxelles, Belgium.

Abstract

Ultraviolet absorption cross-sections of trifluorobromomethane (CF_3Br -Halon 1301), difluoro-dibromomethane (CF_2Br_2 -Halon 1202) and of difluoro-bromo-chloromethane (CF_2BrCl -Halon 1211) are measured in the wavelength interval 172-304 nm for temperatures ranging from 210 to 295 K with uncertainties between 2 and 4 %. They are compared with previous measurements available at room temperature. Temperature effects are discussed and parametrical formulae are proposed to compute the absorption cross-sections for wavelengths and temperatures useful in atmospheric modelling calculations. Photodissociation coefficients are presented and their temperature dependence is discussed.

Résumé

Les sections efficaces d'absorption des trifluoro-bromo-méthane (CF_3Br -Halon 1301), difluoro-dibromo-méthane (CF_2Br_2 -Halon 1202) et difluoro-bromo-chloro-méthane (CF_2BrCl -Halon 1211) ont été mesurées entre 172 et 304 nm pour des températures variant de 210 à 295 K, avec un coefficient d'incertitude compris entre 2 et 4 %. Ces valeurs sont comparées avec des déterminations antérieures obtenues à température ambiante. Les effets de température sont discutés et des équations paramétriques sont proposées afin de calculer les valeurs de sections efficaces d'absorption dans les domaines de longueur d'onde et de température utiles aux modélisations atmosphériques. Les coefficients de photodissociation sont présentés et leur dépendance vis à vis de la température est discutée.

Samenvatting

De werkzame absorptiedoorsneden van bromotrifluormethaan (CF_3Br -halon 1301), dibromodifluormethaan (CF_2Br_2 -halon 1202) en bromochloordifluormethaan (CF_2BrCl -halon 1211) werden gemeten tussen 172 en 304 nm, in het temperatuurgebied 210-295 K, met onzekerheden tussen 2 en 4%. Ze worden vergeleken met vorige metingen die bij kamertemperatuur bekomen werden. De temperatuureffecten worden besproken en parametrische formules worden gegeven die toelaten waarden van werkzame absorptiedoorsneden voor gegeven golflengten en temperaturen af te leiden. De fotodissociatie coëfficiënten worden gegeven en hun temperatuurafhankelijkheid wordt besproken.

Zusammenfassung

Die effektiver Absorptionsquerschnitten von Bromotrifluormethan (CF_3Br -Halon 1301), Dibromodifluormethan (CF_2Br_2 -Halon 1202) und Bromochloordifluormethan (CF_2BrCl -Halon 1211) wurden gemessen zwischen 172 und 304 nm, für Temperaturen zwischen 210 und 295 K, mit einer 2-4% Unsicherheit. Diese Daten werden verglichen mit vorigen Bestimmungen bei Zimmertemperatur. Die Temperatureffekten werden besprochen und parametrische Vergleichen, die zulassen Werten zu berechnen von Absorptionsquerschnitten für gegeben Wellenlänge und Temperaturen, werden gegeben. Die Fotodissoziationskoeffizienten werden bestimmt und die Temperaturabhängigkeit wird diskutiert.

INTRODUCTION

Recent studies (Prather et al., 1984; Rodriguez et al., 1986; Yung et al., 1980) show that brominated compounds can play a significant role in the ozone catalytic destruction in the stratosphere. RBr species concentrations have been measured in the atmosphere by several authors (Fabian et al., 1981; Lal et al., 1985; Cicerone et al., 1988; Berg et al., 1984; Penkett et al., 1985; Class et al., 1986) confirming their possible impact on the ozone layer. The values of the ozone depletion efficiency relative to CFC-11 are, at the present time, estimated to be included between 10 and 11.4 for Halon 1301 and between 2.7 and 3.0 for the Halon 1211 (Brasseur and Simon, 1988).

The reliability of models is strongly dependent on the photodissociation pattern adopted for these bromocarbons. Until now, one set of measurements of absorption cross-sections is available at room temperature for most of the bromocarbons (Molina et al., 1982).

The purpose of this paper is to report a new investigation of ultraviolet absorption cross-sections of three brominated methanes (CF_3Br , CF_2Br_2 and CF_2BrCl) measured between 172 and 300 nm, for temperatures between 295 and 210 K. Temperature dependence of absorption cross-section is clearly demonstrated. Photodissociation coefficients are calculated and their temperature dependence is discussed.

EXPERIMENTAL

The absorption measurements have been performed by means of a single beam experimental device previously described (Gillotay and Simon, 1988) including a Deuterium or a Tungsten filament light source, a 1 m McPherson 225 monochromator, a 2 m thermostat absorption cell and a EMR type 542 P-09-18 solar blind photomultiplier. The temperature is regulated down to 210 K by circulation of cooled methylcyclohexane through a double jacket around the absorption cell and is determined with a precision better than 1 % at 210 K. The pressures ranging from 2×10^{-3}

to 1000 torr are measured with three capacitance manometers (MKS-Baratron) with a precision better than 0.1 %.

Determination of absorption cross-sections is made after at least fifteen sequential recordings of the incident and absorbed fluxes measured for identical temperature conditions, using the Beer-Lambert's law.

The three "Halon" provided by Kali Chemie were of analytical grade and used after vacuum distillations and thorough outgassing. The gas phase chromatography does not reveal any impurities with concentration greater than 0.1 % .

RESULTS

Numerical values of absorption cross-sections for selected wavelengths between 168 and 304 nm (2 nm intervals) and wavenumber intervals of 500 cm^{-1} currently used for aeronomy modelling (Brasseur and Simon, 1981) are respectively given in Tables 2a-4a and 2b-4b. The absorption spectra are illustrated in Figures 1-6.

Ambient Temperature (295K)

At ambient temperature, the measurements have been performed at working pressures given in Table 1. In all cases, the Beer-Lambert's law was found to hold for absorptions ranging from 10 to 85 %. In such conditions, and according to the error budget recently published by Simon et al., (1988), the absorption cross-sections given in Tables 2-4 are determined with an accuracy of ± 2 %.

The absorption cross-section measurements of CF_3Br , which have been extended down to 168 nm, are illustrated in Figure 1 and display a continuous absorption spectrum with a maximum around 206 nm and cross-section values ranging from $1.3 \times 10^{-19} \text{ cm}^2 \text{ molec}^{-1}$ at 206 nm to $6 \times 10^{-24} \text{ cm}^2 \text{ molec}^{-1}$ at 280 nm. Comparison with the only available set of

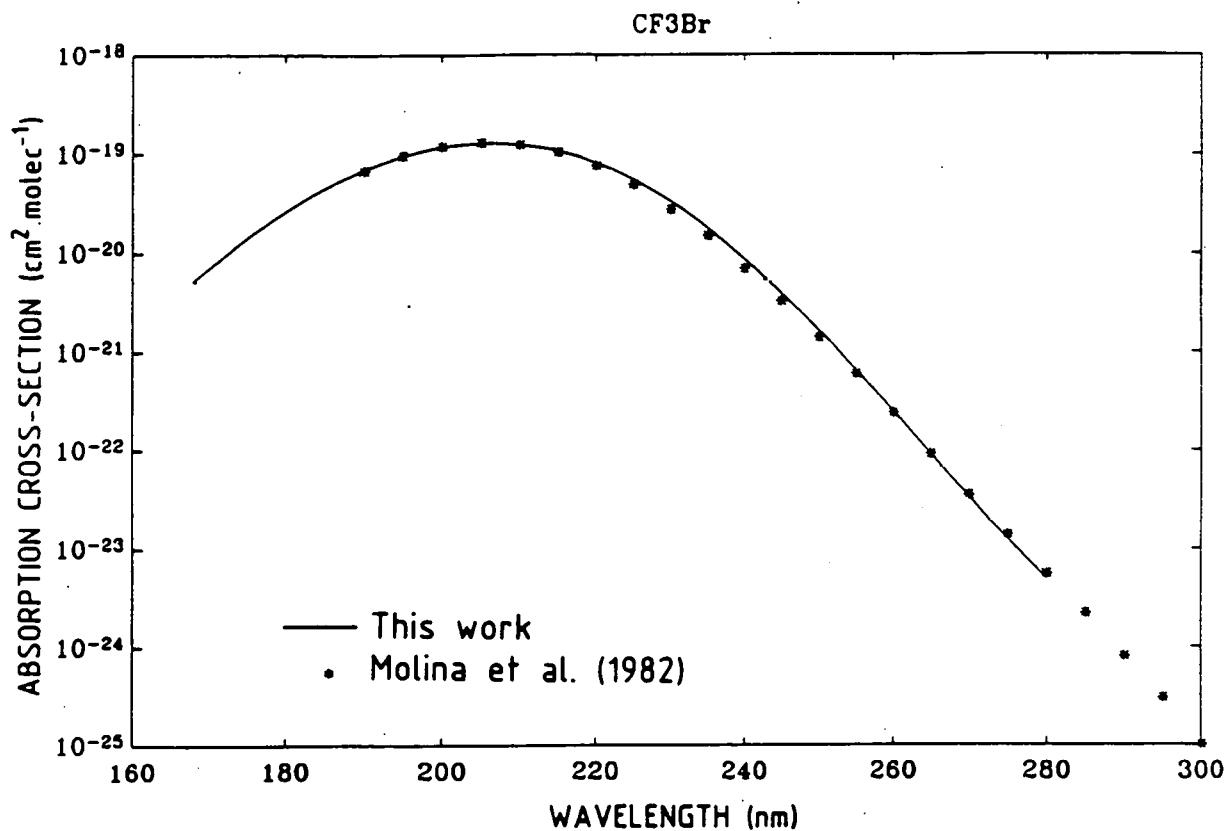


Fig. 1. : Ultraviolet absorption cross-sections of CF₃Br at 295 K, between 170 and 300 nm.

measurements published by Molina et al. (1982) show a good agreement (within the experimental accuracy) between 190 and 225 nm and for wavelengths greater than 255 nm. Between 225 and 255 nm, the values proposed by Molina et al (1982) are in average 15 % lower than those reported here, excepted for one measurement at 240 nm for which the difference reaches 34 %.

CF_2Br_2 displays a continuous absorption spectrum with two maxima (respectively at 188 and 225 nm) with cross-sections values ranging from $2.5 \times 10^{-18} \text{ cm}^2 \text{ molec}^{-1}$ to $1.8 \times 10^{-22} \text{ cm}^2 \text{ molec}^{-1}$ at 304 nm, (Figure 2). Comparison with the values previously published by Molina et al. (1982) show a good agreement over the all spectral range excepted between 240 and 260 where the differences can reach a maximum of 10 %.

For CF_2BrCl , as shown by Figure 3., a continuous absorption spectrum is also observed between 168 and 302 nm with a maximum at 204 nm and cross-section values ranging from $1.2 \times 10^{-18} \text{ cm}^2 \text{ molec}^{-1}$ at the maximum to $2.5 \times 10^{-23} \text{ cm}^2 \text{ molec}^{-1}$ at 302 nm. In this case, the values proposed by Molina et al. (1982) are in average 20-25 % lower than those reported here over the whole spectral range excepted for wavelengths greater than 295 nm.

The differences between the two sets of measurements are difficult to explain in terms of their accuracy. The purity of the compounds used in this work has been carefully checked (see section "experimental"). There is no indication of the level and the nature of impurities in the products used by Molina et al. (1982).

Low Temperature (210-270K)

Absorption cross-sections have been measured at three temperatures in the greatest range of pressure afforded by the vapor pressure conditions. The experimental conditions are summarized in table 1. The accuracy is ± 3.5 % according to the error budget published by Simon et al. (1988). At low temperature, as can be seen on Figures 4-6,

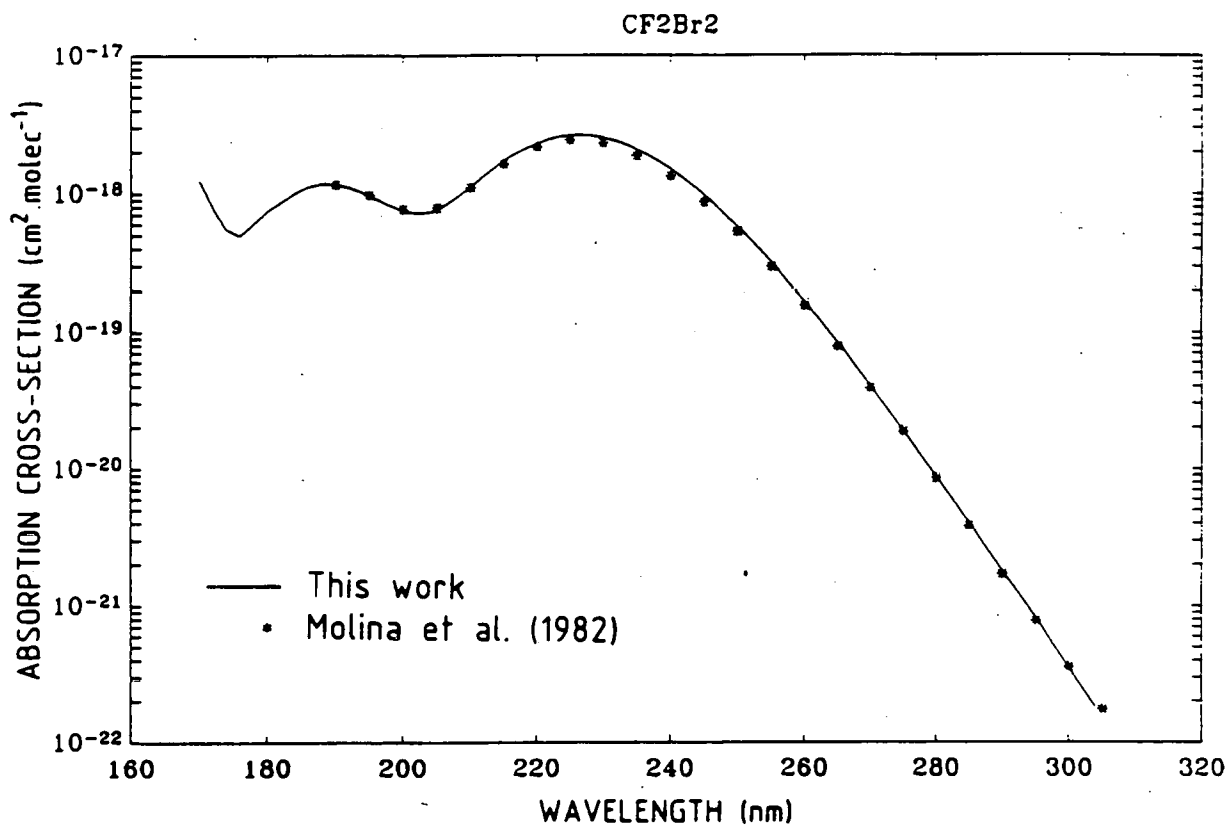


Fig. 2. : Ultraviolet absorption cross-sections of CF₂Br₂ at 295 K, between 170 and 304 nm.

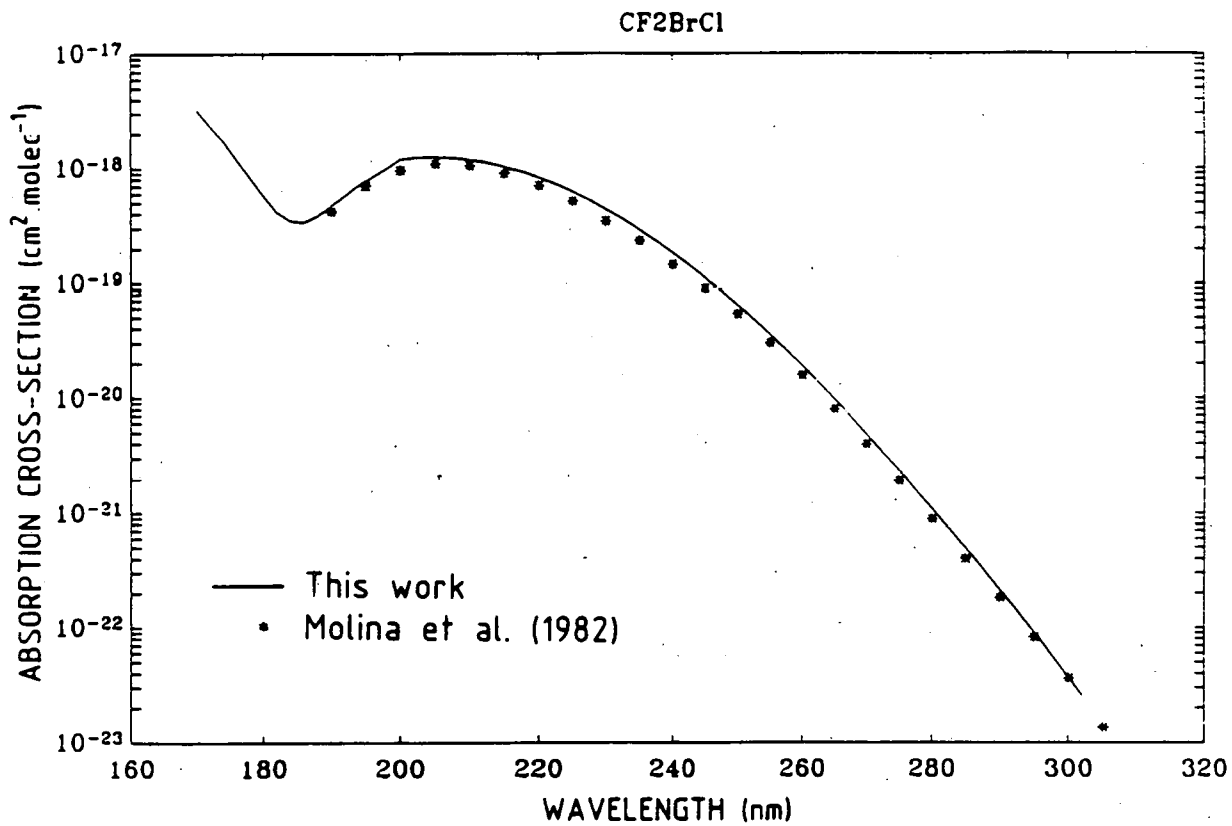


Fig. 3. : Ultraviolet absorption cross-sections of CF₂BrCl at 295 K, between 170 and 302 nm.

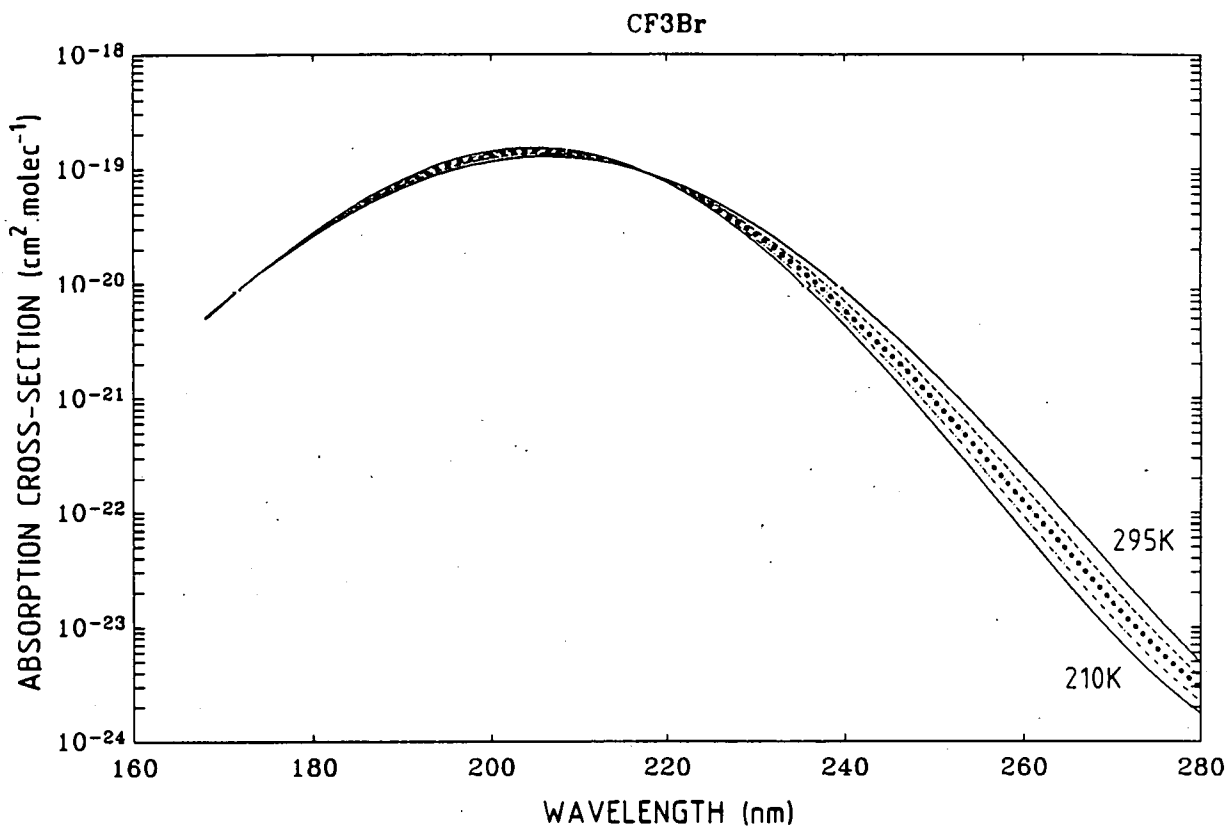


Fig. 4. : Ultraviolet absorption cross-sections of CF₂Br versus wavelength as a function of temperature.
(T = 295, 270, 250, 230, 210 K).

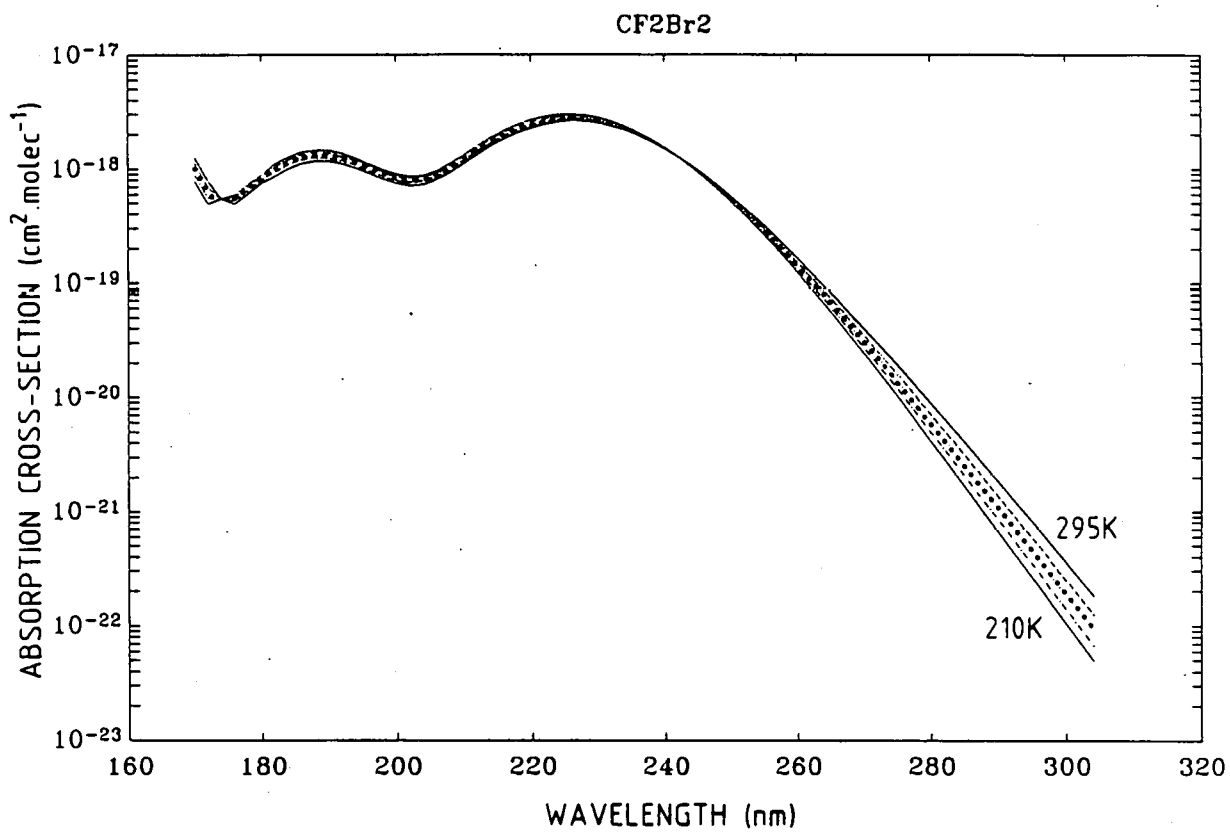


Fig. 5. : Ultraviolet absorption cross-sections of CF_2Br_2 versus wavelength as a function of temperature. (T = 295, 270, 250, 230, 210 K).

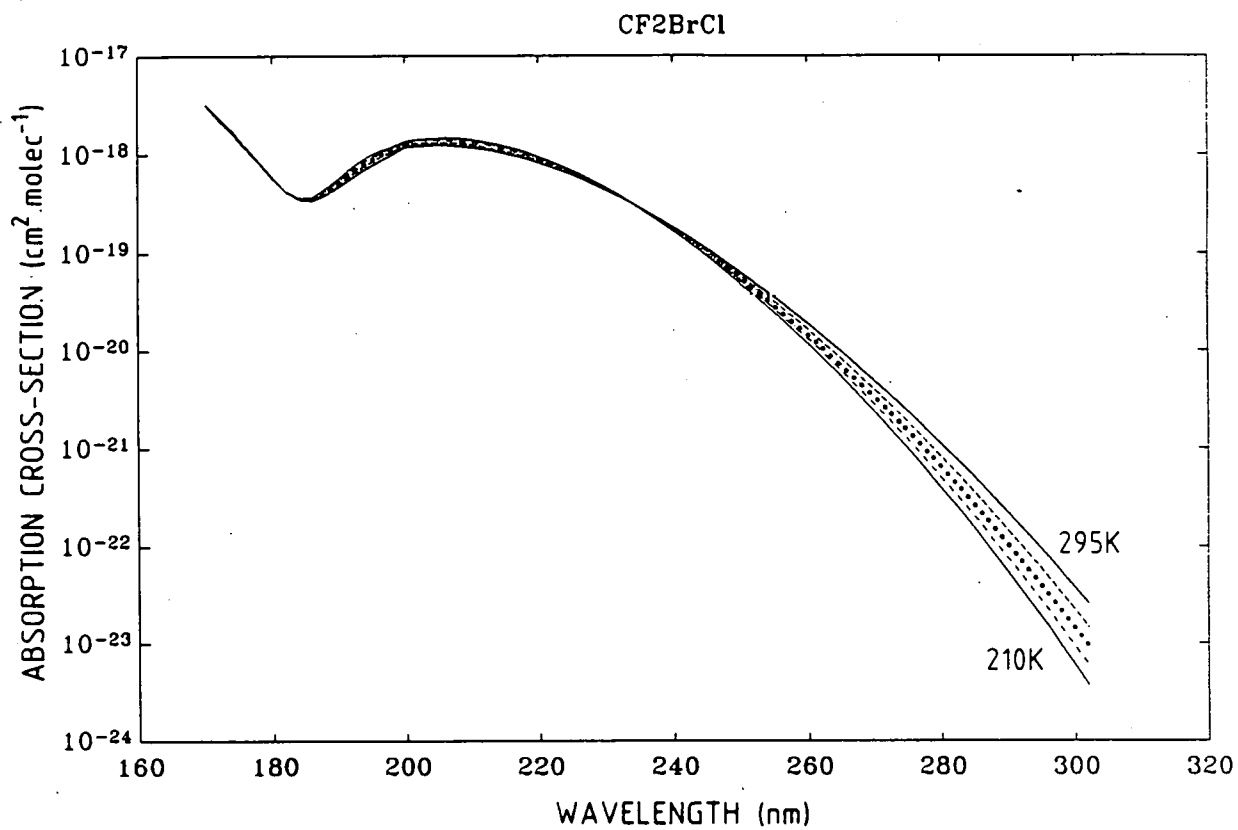


Fig. 6. : Ultraviolet absorption cross-sections of CF_2BrCl versus wavelength as a function of temperature. (T = 295, 270, 250, 230, 210 K).

the absorption cross-sections show a temperature dependence depending on both the wavelength and the chemical composition of the compound. The absorption cross-sections decrease with temperature in the region of the longer wavelengths and increase in the region of the maximum of absorption. These effects are the most significant at the lower temperature.

For the three compounds, the analysis of the relationship of absorption cross-sections versus temperature for a given wavelength shows an exponential dependence on temperature in the all temperature and wavelength ranges considered in this work. Figures 7-9 illustrate this exponential dependence for the longer wavelengths.

Numerical values deduced from a least square fit through the three temperatures measured are presented in tables 2-4 for five defined temperatures (295, 270, 250, 230, 210K) which cover the usual atmospheric temperature conditions.

As explained above, the absorption cross-sections can be represented by an empirical function of temperature for each wavelength according to the following expression :

$$\log_{10} \sigma(\lambda) = A(\lambda) + B(\lambda) \times T \quad (1)$$

where parameters A and B were determined by a polynomial least square fit of the available experimental data with respect to temperature and wavelength to obtain the following polynomial expression :

$$\log_{10} \sigma(\lambda, T) = A_0 + A_1 \lambda + \dots + A_n \lambda^n + (T-273) \times (B_0 + B_1 \lambda + \dots + B_n \lambda^n) \quad (2)$$

The computed values of A and B are given in table 5. The values of absorption cross-sections calculated with expression (2) represent all the experimental data with differences lower than $\pm 4\%$.

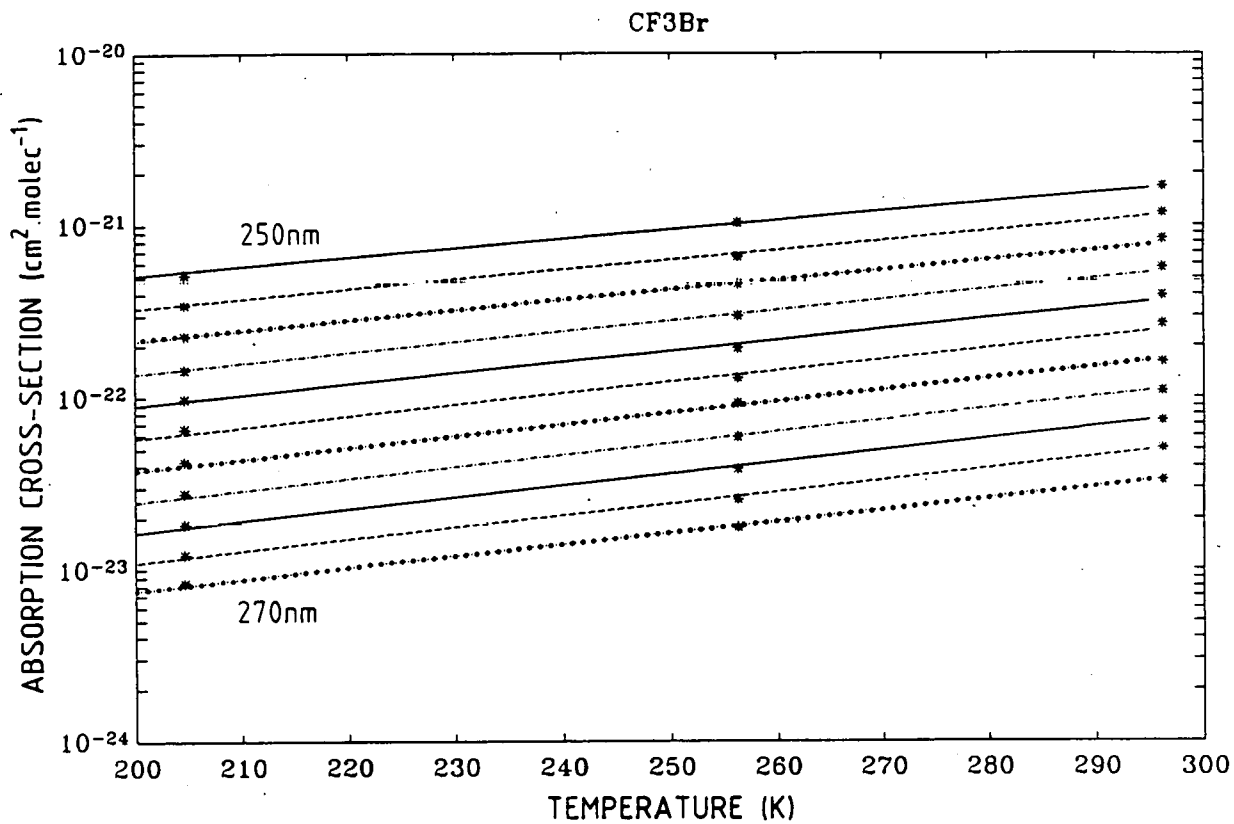


Fig. 7. : Ultraviolet absorption cross-sections of CF₃Br, between 250 and 270 nm, versus temperature.
Wavelength increment between successive curves is 2 nm.

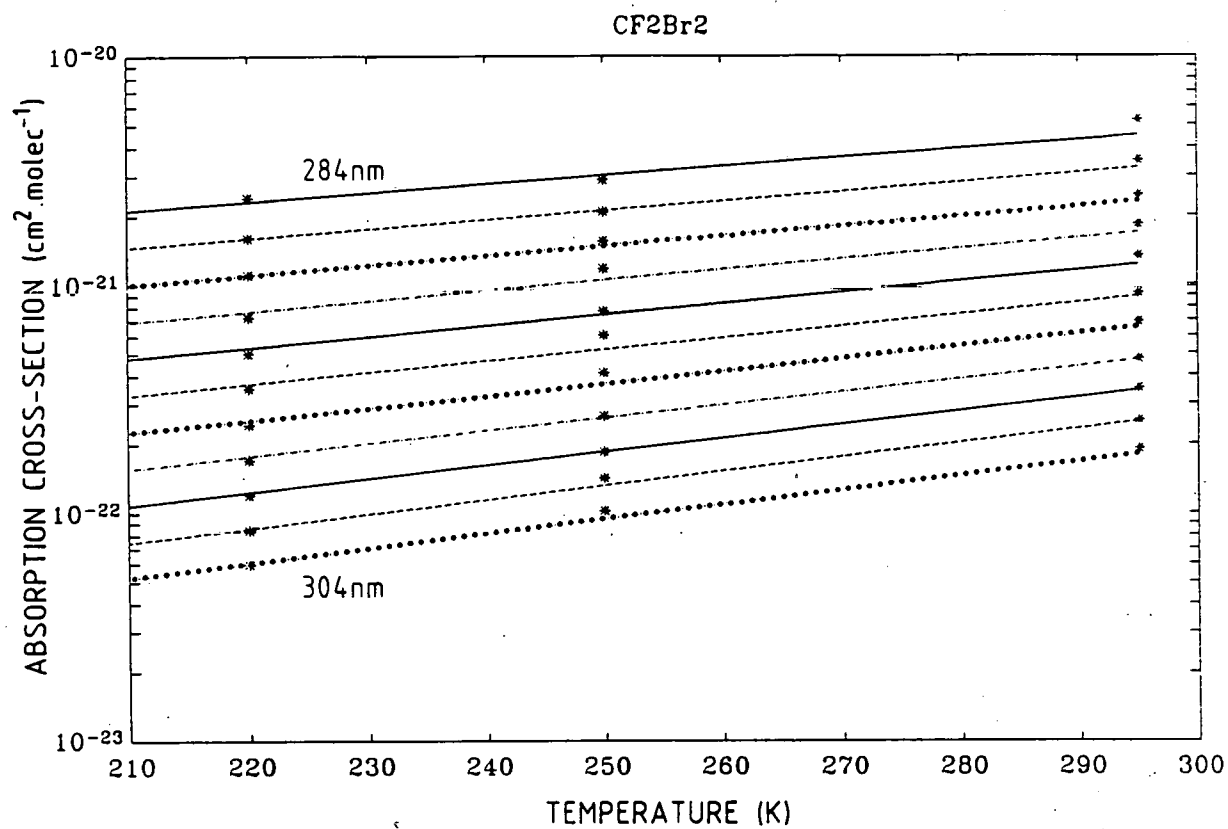


Fig. 8. : Ultraviolet absorption cross-sections of CF_2Br_2 , between 284 and 304 nm, versus temperature. Wavelength increment between successive curves is 2 nm.

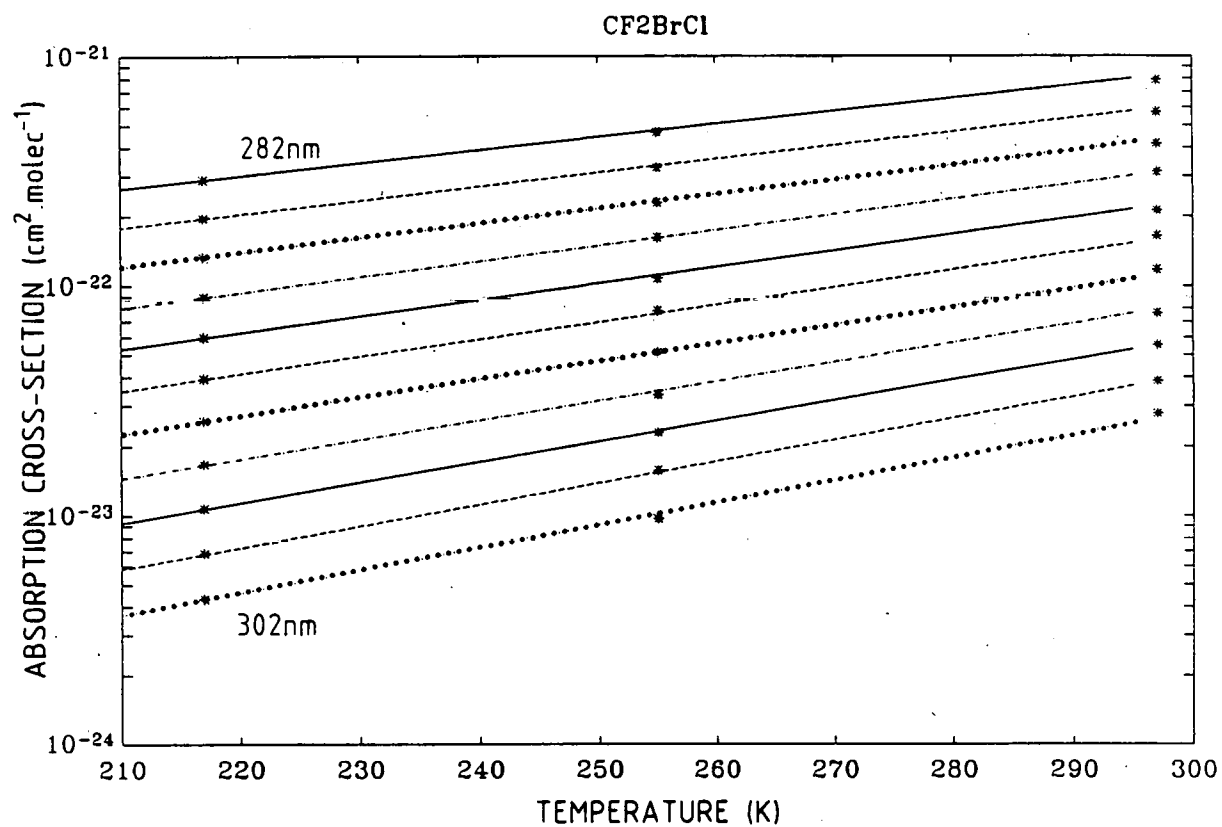


Fig. 9. : Ultraviolet absorption cross-sections of CF₂BrCl, between 282 and 302 nm, versus temperature. Wavelength increment between successive curves is 2 nm.

Relative values of absorption cross-sections $\sigma(T)/\sigma(295)$ versus wavelength relationships, for a given temperature, display very similar features for the three compounds. (Fig 10-12)

DISCUSSION

Photodissociation coefficients J for a given altitude z , zenith angle χ and wavelength interval have been computed according to the relations:

$$J^z = \sigma_\lambda q_\lambda(z)$$

$$q_\lambda(z) = q_\lambda(\infty) e^{-\tau_\lambda(z)}$$

$$\tau_\lambda(z) = \int_z^\infty [n(O_2)\sigma(O_2) + n(O_3)\sigma(O_3) + n(\text{air})\sigma_{\text{scatt.}}] \sec\chi dz \quad (3)$$

where σ are the absorption cross-sections

$q_\lambda(z)$ and $q_\lambda(\infty)$ are the solar irradiance at altitude z or extraterrestrial ($z = \infty$)

n are the number of particle per volume unit for solar zenith angles of 0° and 60° ($\sec\chi = 1$ and 2), taking the values of $\sigma(O_2)$, $\sigma(O_3)$ from WMO (1985) and Kockarts (1976), of σ_{scatt} from Nicolet (1984) and the values of $q_\lambda(\infty)$ from WMO (1985), and taking into account the actual values of cross-sections which correspond to the temperature conditions prevailing at a definite altitude.

A comparison of either temperature dependent or independent photodissociation coefficients for different stratospheric altitudes (15 to 50 km) is presented in table 6 where relative photodissociation coefficients $J(T)/J(295)$ are given for the studied compounds.

Obviously, the effect is maximum in the mid stratosphere and gradually decreases, following the temperature profile in the stratosphere.

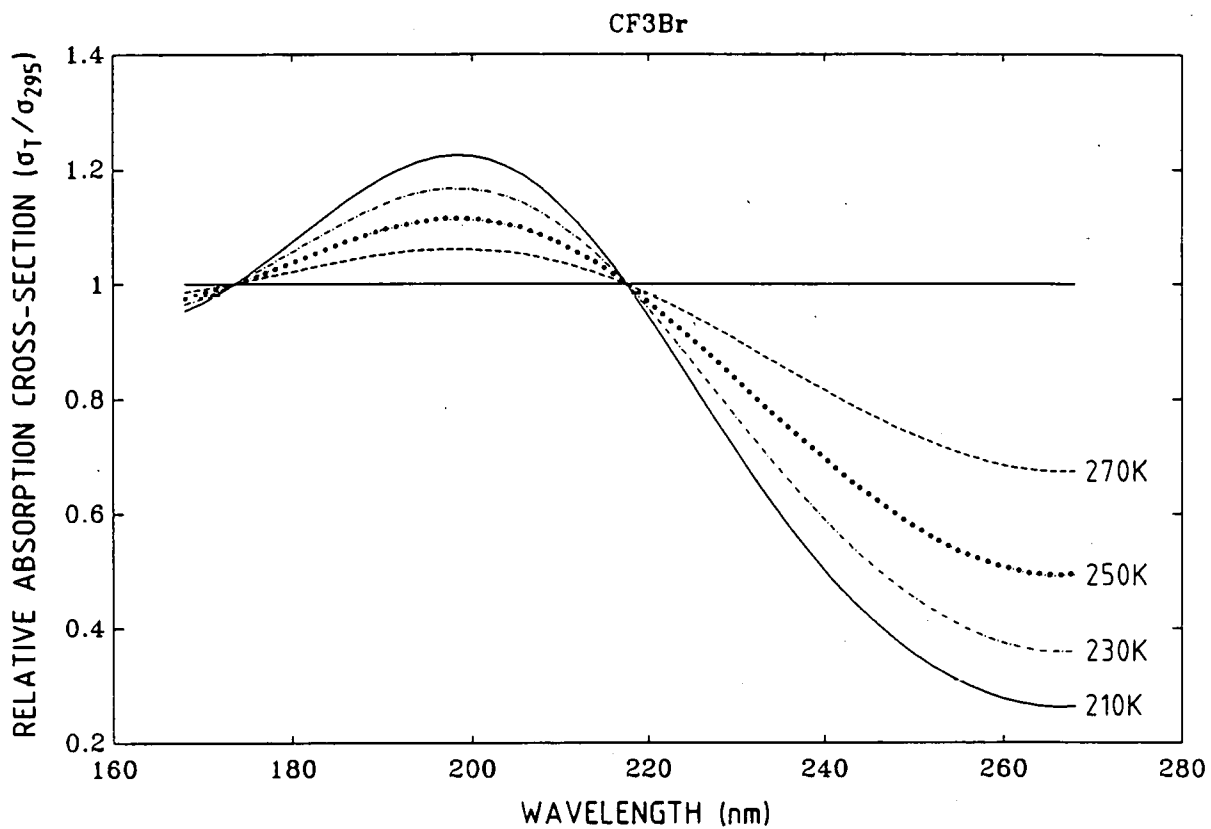


Fig. 10.: Relative absorption cross-sections $\sigma(T)/\sigma(295 \text{ K})$ of CF₃Br as a function of wavelength.
(T = 270K, 250K, 230K and 210K).

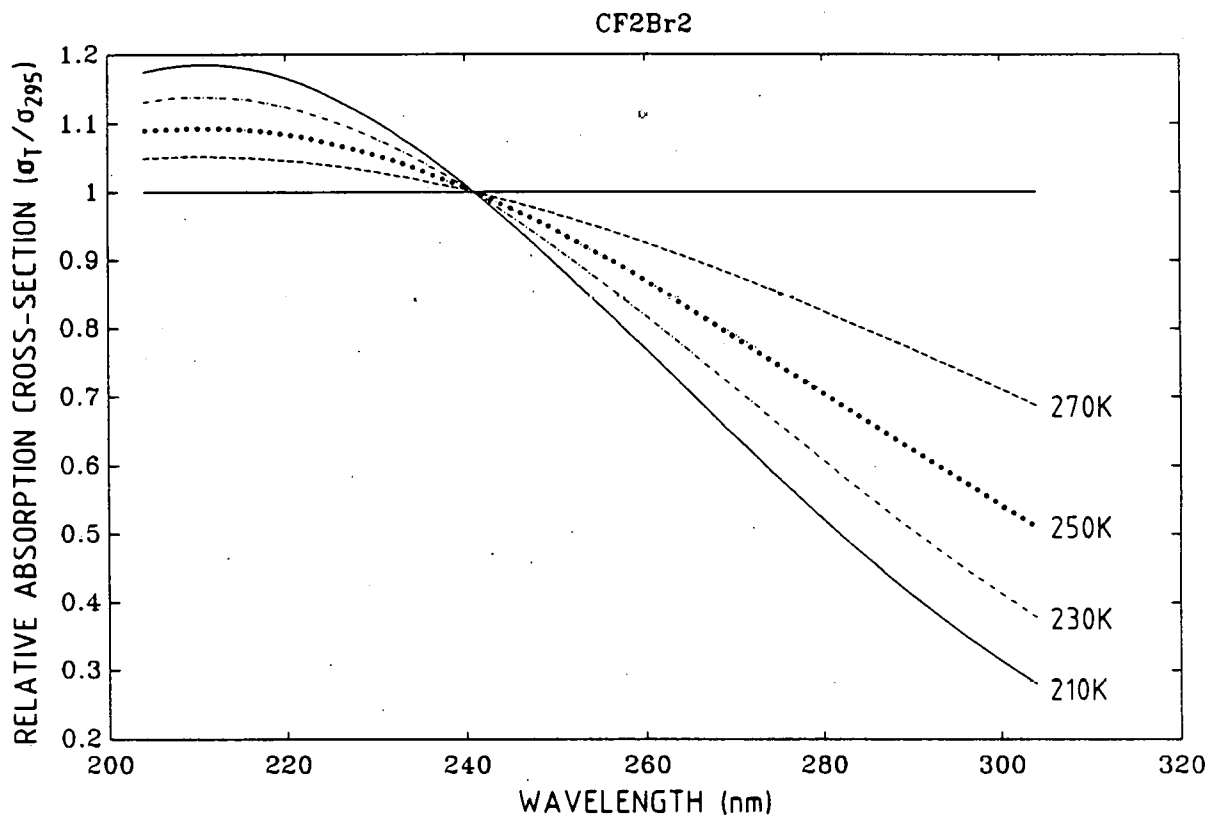


Fig. 11.: Relative absorption cross-sections $\sigma(T)/\sigma(295\text{ K})$ of CF_2Br_2 as a function of wavelength.
 (T = 270K, 250K, 230K and 210K).

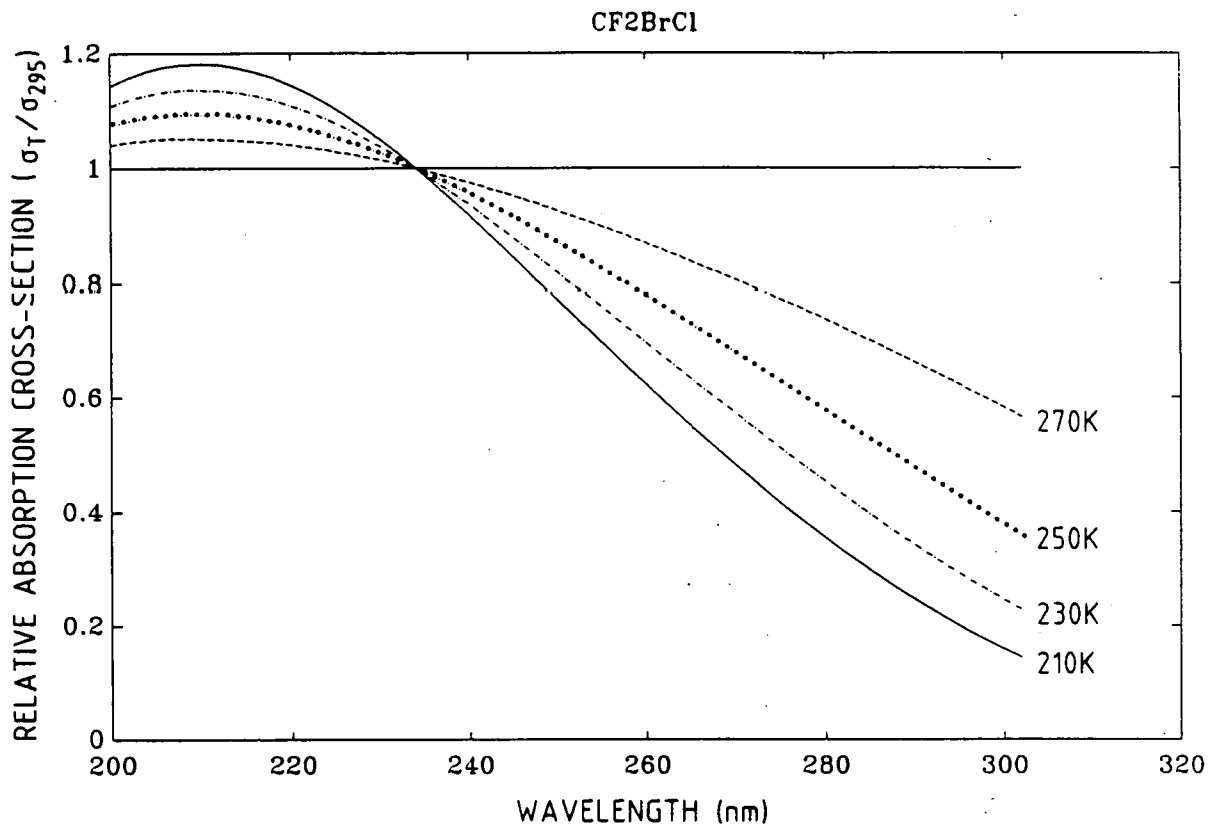


Fig. 12.: Relative absorption cross-sections $\sigma(T)/\sigma(295 \text{ K})$ of CF₂BrCl as a function of wavelength.
(T = 270K, 250K, 230K and 210K).

Due to the significant increase of ozone optical depth in the stratosphere at wavelength beyond 220 nm, the value of the overall photodissociation coefficients between 15 and 35 km is mainly influenced by the 200-210 nm interval contribution. In such conditions, a significant increase of overall photodissociation coefficients is to be expected because of the strong increase of absorption cross-sections (up to 25%) at lower temperatures in this wavelength interval.

The introduction of higher photodissociation coefficients in atmospheric models decreases altitudes of photolysis, and therefore changes the altitude profile of the considered halomethane in the stratosphere.

Calculations have also been made for the troposphere, between 0 to 14 km altitudes. To perform these calculations, the values of the absorption cross-sections have been extrapolated taking into account an exponential decrease of absorption cross-sections with respect of wavelength. The results, presented in table 7, are in good agreement with the integrated values of the photodissociation coefficients over the all tropospheric range, proposed by Molina et al. 1982.

In conclusion, this work presents a complete and coherent set of experimental data showing a non negligible temperature dependence of the absorption cross-sections and of the photodissociation coefficients of bromo-fluoro-methanes. It gives fairly simple parametrical functions to compute the absorption cross-section values with respect of temperature and wavelength.

ACKNOWLEDGMENTS

The authors wish to thank Dr. G. Brasseur for helpful discussions, Mr. L. Dierickx who performed some of the measurements and Mr. E. Falise who performed the computer calculations of the photodissociation coefficients.

REFERENCES

- BERG, W.W., L.E. HEIDT, W. POLLOCK, P.D. SPERRY, R.J. CICERONE, and E.S. GLADNEY, 1984, Brominated organic species in the Arctic atmosphere, *Geophys. Res. Lett.*, **11**, 429-432.
- BRASSEUR, G. and P.C. SIMON, 1981, Stratospheric and thermal response to long-term variability in solar UV irradiance., *J. Geophys. Res.*, **86**, 7343-7362.
- BRASSEUR, G. and P.C. SIMON, 1988, Changes in stratospheric ozone: observations and theories, *Aeronomica Acta A* 334.
- CLASS, Th., R. KOHNLE, K. BALLSCHMITER, 1986, Chemistry of organic races in air VII : Bromo- and Bromochloromethanes in air over Atlantic Ocean, *Chemosphere*, **15**, 429-436.
- CICERONE, R.J., L.E. HEIDT and W.H. POLLOCK, 1988, Measurements of atmospheric Methyl bromide (CH_3Br) and Bromoform (CHBr_3). *J. Geophys. Res.*, **93**, 3745-3749.
- FABIAN, P., R. BORCHERS, S.A. PENKETT, and N.J.D. PROSSER, 1981, Halocarbons in the stratosphere, *Nature*, **294**, 733-735.
- GILLOTAY, D. and P.C. SIMON, 1988, Ultraviolet absorption cross-sections of methyl bromide at stratospheric temperatures, *Ann. Geophysicae*, **6**, 211-215.
- KOCKARTS, G., 1976, Absorption and Photodissociation in the Schumann-Runge bands of molecular oxygen in the terrestrial atmosphere, *Planet. Space Sci.*, **24**, 589-604.
- LAL, S., R. BORCHERS, P. FABIAN and B.C. KRUGER, 1985, Increasing abundance of CBrClF_2 in the atmosphere, *Nature*, **316**, 135-136.
- MOLINA, L.T., M.J. MOLINA and F.S. ROWLAND, 1982, Ultraviolet absorption cross-sections of several brominated methanes and ethanes of atmospheric interest, *J. Phys. Chem.*, **86**, 2672-2676.
- NICOLET, M., 1984, On the molecular scattering in the terrestrial atmosphere : an empirical formula for calculation in the homosphere, *Planet. Space Sci.*, **32**, 1467-1468.
- PENKETT, S.A., B.M.R. JONES, M.J. RYCROFT and D.A. SIMMONS, 1985, An interhemispheric comparison of the concentrations of bromide compounds in the atmosphere, *Nature*, **318**, 550-553.

- PRATHER, M.J., M.B. McELROY and S.C. WOFYSY, 1984, Reductions in ozone at high concentrations of stratospheric halogens, *Nature*, 312, 227-231.
- RODRIGUEZ, J.M., M.K.M. KO and N.D. SZE, 1986, Chlorine chemistry in the Antarctic stratosphere : Impact of OC10 and Cl2O2 and implications for observations, *Geophys. Res. Lett.*, 13, 1292-1295.
- SIMON, P.C., D. GILLOTAY, N. VANLAETHEM-MEUREE and J. WISEMBERG, 1988, Ultraviolet absorption cross-sections of chloro- and chloro-fluoro-methanes at stratospheric temperatures., *J. Atm. Chem.*, 7, 107-135.
- WMO, 1985, Atmospheric ozone 1985, WMO global ozone research and monitoring project, report 16, vol.I, 355-367.
- YUNG, Y.L., J.P. PINTO, R.T. WATSON, and S.P. SANDER, 1980, Atmospheric bromine and ozone perturbations in the lower stratosphere, *J. Atmos. Sci.*, 37, 339-353.

TABLE 1. : Pressure ranges used for the absorption cross-section measurements.

| | | PRESSURE (torr) | | |
|---------------------------------|-----------|--------------------------|--------------------------|----------------------------|
| Compound | Temp. (K) | 295 K | 255 K | 210 K |
| CF ₃ Br | | 722 - 6x10 ⁻¹ | 597 - 6x10 ⁻¹ | 384.6 - 2x10 ⁻² |
| CF ₂ Br ₂ | | 234 - 3x10 ⁻² | 67 - 1x10 ⁻¹ | 3.4 - 2x10 ⁻² |
| CF ₂ BrCl | | 453 - 1x10 ⁻¹ | 80 - 8x10 ⁻² | 10.3 - 9x10 ⁻² |

TABLE 2a : Absorption cross-sections of CF₃Br at 2 nm intervals for five selected temperatures (295, 270, 250, 230, and 210K)

$\sigma(\lambda) \times 10^{21}$ (cm² molec.⁻¹)

| λ (nm) | 295 K | 270K | 250K | 230K | 210K |
|----------------|-------|------|------|------|------|
| 168 | 5.17 | 5.09 | 5.04 | 4.98 | 4.93 |
| 170 | 6.96 | 6.89 | 6.84 | 6.79 | 6.73 |
| 172 | 9.28 | 9.24 | 9.21 | 9.17 | 9.14 |
| 174 | 12.2 | 12.3 | 12.3 | 12.3 | 12.3 |
| 176 | 16.0 | 16.1 | 16.2 | 16.3 | 16.4 |
| 178 | 20.5 | 20.8 | 21.1 | 21.3 | 21.6 |
| 180 | 26.1 | 26.6 | 27.1 | 27.5 | 28.0 |
| 182 | 32.6 | 33.5 | 34.3 | 35.0 | 35.8 |
| 184 | 40.2 | 41.6 | 42.7 | 43.9 | 45.1 |
| 186 | 48.8 | 50.8 | 52.4 | 54.1 | 55.9 |
| 188 | 58.2 | 60.9 | 63.2 | 65.5 | 67.9 |
| 190 | 68.4 | 71.9 | 74.8 | 77.8 | 81.0 |
| 192 | 78.8 | 83.2 | 86.9 | 90.7 | 94.7 |
| 194 | 89.3 | 94.6 | 99.0 | 104 | 108 |
| 196 | 99.4 | 105 | 110 | 116 | 121 |
| 198 | 109 | 115 | 121 | 127 | 133 |
| 200 | 116 | 123 | 129 | 136 | 142 |
| 202 | 122 | 130 | 136 | 142 | 149 |
| 204 | 126 | 133 | 139 | 146 | 152 |
| 206 | 128 | 134 | 140 | 146 | 152 |
| 208 | 127 | 132 | 137 | 142 | 148 |
| 210 | 123 | 128 | 132 | 136 | 140 |
| 212 | 117 | 121 | 124 | 127 | 130 |
| 214 | 110 | 112 | 114 | 116 | 118 |
| 216 | 101 | 102 | 102 | 103 | 104 |
| 218 | 90.6 | 90.3 | 90.1 | 89.9 | 89.7 |
| 220 | 79.9 | 78.6 | 77.6 | 76.6 | 75.6 |
| 222 | 69.2 | 67.1 | 65.4 | 63.8 | 62.3 |
| 224 | 58.8 | 56.1 | 54.1 | 52.1 | 50.1 |
| 226 | 49.1 | 46.1 | 43.8 | 41.6 | 39.5 |
| 228 | 40.3 | 37.1 | 34.7 | 32.5 | 30.5 |
| 230 | 32.4 | 29.3 | 27.0 | 25.0 | 23.0 |
| 232 | 25.7 | 22.8 | 20.7 | 18.8 | 17.1 |
| 234 | 20.0 | 17.4 | 15.6 | 13.9 | 12.4 |
| 236 | 15.3 | 13.1 | 11.5 | 10.1 | 8.88 |

TABLE 2a (cont.)

| λ (nm) | 295 K | 270K | 250K | 230K | 210K |
|----------------|---------|---------|---------|---------|---------|
| 238 | 11.6 | 9.66 | 8.35 | 7.22 | 6.24 |
| 240 | 8.62 | 7.04 | 5.98 | 5.09 | 4.33 |
| 242 | 6.33 | 5.06 | 4.23 | 3.54 | 2.96 |
| 244 | 4.59 | 3.59 | 2.95 | 2.43 | 2.00 |
| 246 | 3.28 | 2.52 | 2.04 | 1.65 | 1.33 |
| 248 | 2.32 | 1.75 | 1.39 | 1.11 | 0.881 |
| 250 | 1.63 | 1.20 | 0.941 | 0.738 | 0.579 |
| 252 | 1.13 | 0.818 | 0.632 | 0.489 | 0.378 |
| 254 | 0.777 | 0.554 | 0.422 | 0.322 | 0.246 |
| 256 | 0.530 | 0.373 | 0.281 | 0.212 | 0.160 |
| 258 | 0.360 | 0.250 | 0.186 | 0.139 | 0.104 |
| 260 | 0.243 | 0.167 | 0.123 | 0.0911 | 0.0674 |
| 262 | 0.164 | 0.111 | 0.0817 | 0.0600 | 0.0440 |
| 264 | 0.110 | 0.0742 | 0.0542 | 0.0396 | 0.0290 |
| 266 | 0.0736 | 0.0496 | 0.0362 | 0.0264 | 0.0192 |
| 268 | 0.0494 | 0.0333 | 0.0243 | 0.0177 | 0.0129 |
| 270 | 0.0331 | 0.0225 | 0.0164 | 0.0120 | 0.00882 |
| 272 | 0.0223 | 0.0153 | 0.0112 | 0.00829 | 0.00611 |
| 274 | 0.0151 | 0.0105 | 0.00779 | 0.00580 | 0.00432 |
| 276 | 0.0103 | 0.00725 | 0.00547 | 0.00414 | 0.00313 |
| 278 | 0.00706 | 0.00509 | 0.00392 | 0.00301 | 0.00232 |
| 280 | 0.00489 | 0.00363 | 0.00286 | 0.00225 | 0.00177 |

TABLE 2b : Absorption cross-sections of CF₃Br averaged over the spectral intervals used in atmospheric modelling calculations for five selected temperatures (295, 270, 250, 230, and 210K)

(wavenumber intervals : 500 cm⁻¹)

$\sigma(\lambda) \times 10^{21}$ (cm² molec.⁻¹)

| N° | λ (nm) | 295K | 270K | 250K | 230K | 210K |
|----|----------------|------|------|------|------|------|
| 43 | 169.5-172.4 | 7.99 | 7.93 | 7.88 | 7.84 | 7.79 |
| 44 | 172.4-173.9 | 10.9 | 10.9 | 10.9 | 10.9 | 10.9 |
| 45 | 173.9-175.4 | 13.4 | 13.4 | 13.4 | 13.5 | 13.5 |
| 46 | 175.4-177.0 | 16.4 | 16.5 | 16.6 | 16.7 | 16.8 |
| 47 | 177.0-178.6 | 20.0 | 20.3 | 20.5 | 20.8 | 21.0 |
| 48 | 178.6-180.2 | 24.3 | 24.8 | 25.2 | 25.5 | 25.9 |
| 49 | 180.2-181.8 | 29.2 | 29.9 | 30.5 | 31.1 | 31.7 |
| 50 | 181.8-183.5 | 35.0 | 36.0 | 36.9 | 37.8 | 38.7 |
| 51 | 183.5-185.2 | 41.6 | 43.1 | 44.4 | 45.6 | 46.9 |
| 52 | 185.2-186.9 | 49.0 | 51.0 | 52.7 | 54.4 | 56.2 |
| 53 | 186.9-188.7 | 57.3 | 59.9 | 62.1 | 64.3 | 66.7 |
| 54 | 188.7-190.5 | 65.8 | 69.1 | 71.8 | 74.7 | 77.7 |
| 55 | 190.5-192.3 | 75.7 | 79.8 | 83.2 | 86.8 | 90.6 |
| 56 | 192.3-194.2 | 85.4 | 90.3 | 94.5 | 98.8 | 103 |
| 57 | 194.2-196.1 | 95.2 | 101 | 106 | 111 | 116 |
| 58 | 196.1-198.0 | 104 | 111 | 116 | 122 | 128 |
| 59 | 198.0-200.0 | 113 | 120 | 125 | 132 | 138 |
| 60 | 200.0-202.0 | 120 | 127 | 133 | 139 | 146 |
| 61 | 202.0-204.1 | 125 | 132 | 138 | 144 | 151 |
| 62 | 204.1-206.2 | 127 | 134 | 140 | 146 | 152 |
| 63 | 206.2-208.3 | 127 | 133 | 139 | 144 | 150 |
| 64 | 208.3-210.5 | 124 | 130 | 134 | 138 | 143 |
| 65 | 210.5-212.8 | 119 | 122 | 125 | 129 | 132 |
| 66 | 212.8-215.0 | 110 | 113 | 114 | 116 | 118 |
| 67 | 215.0-217.4 | 99.7 | 101 | 101 | 102 | 103 |
| 68 | 217.4-219.8 | 87.4 | 86.8 | 86.4 | 85.9 | 85.4 |
| 69 | 219.8-222.2 | 74.6 | 72.8 | 71.5 | 70.1 | 68.8 |
| 70 | 222.2-224.7 | 61.6 | 59.1 | 57.1 | 55.2 | 53.3 |
| 71 | 224.7-227.3 | 49.1 | 46.1 | 43.8 | 41.6 | 39.5 |
| 72 | 227.3-229.9 | 37.8 | 34.6 | 32.3 | 30.1 | 28.1 |
| 73 | 229.9-232.6 | 28.1 | 25.4 | 22.9 | 20.9 | 19.1 |
| 74 | 232.6-235.3 | 20.1 | 17.5 | 15.7 | 14.0 | 12.5 |
| 75 | 235.3-238.1 | 13.9 | 11.8 | 10.3 | 8.99 | 7.86 |
| 76 | 238.1-241.0 | 9.29 | 7.63 | 6.51 | 5.56 | 4.75 |

TABLE 2b (continued)

| N° | λ (nm) | 295K | 270K | 250K | 230K | 210K |
|----|----------------|---------|---------|---------|---------|---------|
| 77 | 241.0-243.9 | 5.89 | 4.69 | 3.90 | 3.25 | 2.71 |
| 78 | 243.9-246.9 | 3.63 | 2.80 | 2.28 | 1.85 | 1.51 |
| 79 | 246.9-250.0 | 2.13 | 1.59 | 1.26 | 1.00 | 0.794 |
| 80 | 250.0-253.2 | 1.24 | 0.901 | 0.699 | 0.542 | 0.421 |
| 81 | 253.2-256.4 | 0.667 | 0.473 | 0.359 | 0.272 | 0.207 |
| 82 | 256.4-259.7 | 0.360 | 0.250 | 0.186 | 0.139 | 0.104 |
| 83 | 259.7-263.2 | 0.181 | 0.123 | 0.0905 | 0.0666 | 0.0490 |
| 84 | 263.2-266.7 | 0.0899 | 0.0607 | 0.0443 | 0.0323 | 0.0236 |
| 85 | 266.7-270.3 | 0.0447 | 0.0301 | 0.0220 | 0.0161 | 0.0117 |
| 86 | 270.3-274.0 | 0.0219 | 0.0150 | 0.0110 | 0.00814 | 0.00600 |
| 87 | 274.0-277.8 | 0.0105 | 0.00738 | 0.00557 | 0.00421 | 0.00317 |
| 88 | 277.8-281.7 | 0.00507 | 0.00375 | 0.00294 | 0.00231 | 0.00182 |

TABLE 3a : Absorption cross-sections of CF_2Br_2 at 2 nm intervals for five selected temperatures (295, 270, 250, 230, and 210K).

| $\lambda(\text{nm})$ | $\sigma(\lambda) \times 10^{21} (\text{cm}^2 \text{ molec.}^{-1})$ | | | | |
|----------------------|--|-------|-------|-------|-------|
| | 295 K | 270 K | 250 K | 230 K | 210 K |
| 170 | 1245 | 1108 | 1000 | 891 | 782 |
| 172 | 781 | 696 | 629 | 560 | 493 |
| 174 | 553 | 551 | 550 | 549 | 548 |
| 176 | 495 | 523 | 546 | 568 | 590 |
| 178 | 603 | 641 | 671 | 700 | 730 |
| 180 | 750 | 791 | 824 | 857 | 890 |
| 182 | 866 | 939 | 997 | 1056 | 1114 |
| 184 | 1009 | 1086 | 1148 | 1210 | 1272 |
| 186 | 1118 | 1204 | 1272 | 1341 | 1409 |
| 188 | 1180 | 1262 | 1327 | 1392 | 1458 |
| 190 | 1168 | 1252 | 1319 | 1387 | 1454 |
| 192 | 1109 | 1185 | 1245 | 1306 | 1366 |
| 194 | 1022 | 1085 | 1135 | 1185 | 1235 |
| 196 | 920 | 973 | 1016 | 1058 | 1100 |
| 198 | 825 | 869 | 905 | 941 | 976 |
| 200 | 748 | 792 | 827 | 862 | 898 |
| 202 | 716 | 758 | 791 | 825 | 858 |
| 204 | 735 | 778 | 812 | 846 | 880 |
| 206 | 810 | 853 | 887 | 921 | 955 |
| 208 | 936 | 989 | 1033 | 1076 | 1119 |
| 210 | 1110 | 1173 | 1223 | 1273 | 1323 |
| 212 | 1431 | 1408 | 1466 | 1525 | 1583 |
| 214 | 1586 | 1670 | 1738 | 1806 | 1873 |
| 216 | 1841 | 1935 | 2011 | 2086 | 2162 |
| 218 | 2081 | 2186 | 2270 | 2353 | 2437 |
| 220 | 2281 | 2394 | 2482 | 2577 | 2676 |
| 222 | 2477 | 2585 | 2675 | 2767 | 2863 |
| 224 | 2540 | 2643 | 2729 | 2817 | 2909 |
| 226 | 2545 | 2640 | 2718 | 2800 | 2883 |
| 228 | 2493 | 2577 | 2646 | 2717 | 2790 |
| 230 | 2390 | 2461 | 2519 | 2578 | 2639 |
| 232 | 2246 | 2302 | 2347 | 2394 | 2442 |
| 234 | 2068 | 2109 | 2143 | 2177 | 2212 |
| 236 | 1869 | 1897 | 1918 | 1941 | 1964 |

TABLE 3a (Cont.)

| λ (nm) | 295K | 270K | 250K | 230K | 210K |
|----------------|-------|-------|--------|--------|--------|
| 238 | 1659 | 1674 | 1686 | 1698 | 1710 |
| 240 | 1448 | 1452 | 1455 | 1459 | 1463 |
| 242 | 1243 | 1238 | 1235 | 1232 | 1229 |
| 244 | 1050 | 1039 | 1031 | 1023 | 1015 |
| 246 | 875 | 860 | 848 | 836 | 825 |
| 248 | 718 | 701 | 687 | 674 | 661 |
| 250 | 582 | 564 | 549 | 535 | 521 |
| 252 | 466 | 447 | 433 | 419 | 406 |
| 254 | 369 | 351 | 337 | 325 | 312 |
| 256 | 289 | 272 | 260 | 248 | 237 |
| 258 | 224 | 209 | 198 | 189 | 178 |
| 260 | 172 | 159 | 150 | 141 | 132 |
| 262 | 130 | 119 | 112 | 104 | 97.3 |
| 264 | 98.7 | 89.6 | 82.9 | 76.7 | 71.0 |
| 266 | 74.0 | 66.5 | 61.0 | 56.0 | 51.3 |
| 268 | 55.1 | 48.9 | 44.5 | 40.5 | 36.8 |
| 270 | 40.8 | 35.9 | 32.3 | 29.1 | 26.3 |
| 272 | 30.1 | 26.1 | 23.3 | 20.8 | 18.6 |
| 274 | 22.1 | 18.9 | 16.7 | 14.8 | 13.1 |
| 276 | 16.1 | 13.7 | 12.0 | 10.5 | 9.17 |
| 278 | 11.7 | 9.81 | 8.51 | 7.38 | 6.39 |
| 280 | 8.52 | 7.04 | 6.04 | 5.18 | 4.44 |
| 282 | 6.17 | 5.03 | 4.27 | 3.62 | 3.08 |
| 284 | 4.47 | 3.59 | 3.02 | 2.53 | 2.13 |
| 286 | 3.23 | 2.56 | 2.13 | 1.77 | 1.47 |
| 288 | 2.34 | 1.83 | 1.50 | 1.23 | 1.01 |
| 290 | 1.69 | 1.30 | 1.06 | 0.856 | 0.695 |
| 292 | 1.22 | 0.928 | 0.744 | 0.596 | 0.478 |
| 294 | 0.876 | 0.663 | 0.525 | 0.415 | 0.329 |
| 296 | 0.645 | 0.474 | 0.370 | 0.290 | 0.226 |
| 298 | 0.470 | 0.340 | 0.262 | 0.202 | 0.156 |
| 300 | 0.343 | 0.244 | 0.186 | 0.142 | 0.108 |
| 302 | 0.252 | 0.176 | 0.132 | 0.0993 | 0.0746 |
| 304 | 0.185 | 0.127 | 0.0944 | 0.0699 | 0.0518 |

TABLE 3b : Absorption cross-sections of CF_2Br_2 averaged over the spectral intervals used in atmospheric modelling calculations for five selected temperatures (295, 270, 250, 230, and 210K)

(wavenumber intervals : 500 cm^{-1})

| N° | $\lambda(\text{nm})$ | $\sigma(\lambda) \times 10^{21} (\text{cm}^2 \text{ molec.}^{-1})$ | | | | |
|----|----------------------|--|------|------|------|------|
| | | 295K | 270K | 250K | 230K | 210K |
| 43 | 169.5-172.4 | 1001 | 870 | 775 | 692 | 602 |
| 44 | 172.4-173.9 | 632 | 602 | 572 | 542 | 513 |
| 45 | 173.9-175.4 | 527 | 535 | 543 | 545 | 552 |
| 46 | 175.4-177.0 | 503 | 538 | 559 | 577 | 601 |
| 47 | 177.0-178.6 | 596 | 631 | 660 | 684 | 703 |
| 48 | 178.6-180.2 | 715 | 752 | 793 | 817 | 847 |
| 49 | 180.2-181.8 | 810 | 861 | 909 | 960 | 1001 |
| 50 | 181.8-183.5 | 912 | 993 | 1040 | 1105 | 1165 |
| 51 | 183.5-185.2 | 1025 | 1103 | 1180 | 1235 | 1300 |
| 52 | 185.2-186.9 | 1120 | 1209 | 1275 | 1343 | 1411 |
| 53 | 186.9-188.7 | 1170 | 1254 | 1324 | 1380 | 1454 |
| 54 | 188.7-190.5 | 1175 | 1253 | 1322 | 1389 | 1455 |
| 55 | 190.5-192.3 | 1115 | 1210 | 1270 | 1337 | 1385 |
| 56 | 192.3-194.2 | 1055 | 1130 | 1175 | 1215 | 1273 |
| 57 | 194.2-196.1 | 970 | 1015 | 1060 | 1100 | 1148 |
| 58 | 196.1-198.0 | 864 | 918 | 952 | 991 | 1035 |
| 59 | 198.0-200.0 | 780 | 827 | 861 | 898 | 922 |
| 60 | 200.0-202.0 | 721 | 768 | 801 | 838 | 872 |
| 61 | 202.0-204.1 | 712 | 768 | 803 | 836 | 869 |
| 62 | 204.1-206.2 | 766 | 824 | 842 | 873 | 915 |
| 63 | 206.2-208.3 | 882 | 932 | 968 | 999 | 1050 |
| 64 | 208.3-210.5 | 1054 | 1112 | 1157 | 1200 | 1250 |
| 65 | 210.5-212.8 | 1285 | 1354 | 1412 | 1476 | 1527 |
| 66 | 212.8-215.0 | 1562 | 1640 | 1714 | 1795 | 1850 |
| 67 | 215.0-217.4 | 1855 | 1952 | 2015 | 2096 | 2175 |
| 68 | 217.4-219.8 | 2144 | 2226 | 2305 | 2399 | 2486 |
| 69 | 219.8-222.2 | 2424 | 2533 | 2623 | 2717 | 2814 |
| 70 | 222.2-224.7 | 2529 | 2634 | 2721 | 2811 | 2904 |
| 71 | 224.7-227.3 | 2545 | 2640 | 2719 | 2800 | 2883 |
| 72 | 227.3-229.9 | 2467 | 2547 | 2613 | 2681 | 2750 |
| 73 | 229.9-232.6 | 2304 | 2366 | 2416 | 2468 | 2520 |
| 74 | 232.6-235.3 | 2073 | 2115 | 2149 | 2183 | 2218 |
| 75 | 235.3-238.1 | 1796 | 1819 | 1838 | 1857 | 1876 |

TABLE 3b (cont.)

| N° | λ (nm) | 295K | 270K | 250K | 230K | 210K |
|----|----------------|-------|--------|--------|--------|--------|
| 76 | 238.1-241.0 | 1500 | 1507 | 1512 | 1518 | 1524 |
| 77 | 241.0-243.9 | 1198 | 1192 | 1188 | 1183 | 1179 |
| 78 | 243.9-246.9 | 925 | 912 | 901 | 890 | 879 |
| 79 | 246.9-250.0 | 682 | 664 | 650 | 637 | 623 |
| 80 | 250.0-253.2 | 493 | 475 | 460 | 446 | 433 |
| 81 | 253.2-256.4 | 335 | 318 | 305 | 292 | 280 |
| 82 | 256.4-259.7 | 224 | 209 | 198 | 188 | 178 |
| 83 | 259.7-263.2 | 140 | 129 | 120 | 113 | 105 |
| 84 | 263.2-266.7 | 85.6 | 77.3 | 71.2 | 65.6 | 60.4 |
| 85 | 266.7-270.3 | 51.2 | 45.3 | 41.1 | 37.3 | 33.9 |
| 86 | 270.3-274.0 | 29.6 | 25.7 | 22.9 | 20.5 | 18.3 |
| 87 | 274.0-277.8 | 16.4 | 13.9 | 12.2 | 10.7 | 9.33 |
| 88 | 277.8-281.7 | 8.80 | 7.27 | 6.25 | 5.37 | 4.61 |
| 89 | 281.7-285.7 | 4.69 | 3.78 | 3.18 | 2.67 | 2.25 |
| 90 | 285.7-289.9 | 2.41 | 1.89 | 1.55 | 1.28 | 1.05 |
| 91 | 289.9-294.1 | 1.22 | 0.928 | 0.744 | 0.596 | 0.478 |
| 92 | 294.1-298.5 | 0.615 | 0.451 | 0.352 | 0.274 | 0.214 |
| 93 | 298.5-303.0 | 0.303 | 0.214 | 0.162 | 0.123 | 0.0930 |
| 94 | 303.0-307.7 | 0.131 | 0.0883 | 0.0644 | 0.0469 | 0.0342 |

TABLE 4a : Absorption cross-sections of CF_2BrCl at 2 nm intervals for five selected temperatures (295, 270, 250, 230, and 210K).

| $\lambda(\text{nm})$ | $\sigma(\lambda) \times 10^{21} (\text{cm}^2 \text{ molec.}^{-1})$ | | | | |
|----------------------|--|-------|-------|-------|-------|
| | 295 K | 270 K | 250 K | 230 K | 210 K |
| 170 | 3230 | 3200 | 3180 | 3160 | 3150 |
| 172 | 2342 | 2300 | 2285 | 2250 | 2227 |
| 174 | 1760 | 1720 | 1680 | 1660 | 1660 |
| 176 | 1209 | 1180 | 1175 | 1170 | 1160 |
| 178 | 847 | 840 | 834 | 830 | 825 |
| 180 | 581 | 580 | 579 | 579 | 578 |
| 182 | 419 | 419 | 418 | 418 | 418 |
| 184 | 350 | 353 | 356 | 359 | 362 |
| 186 | 341 | 347 | 353 | 359 | 366 |
| 188 | 389 | 405 | 420 | 437 | 456 |
| 190 | 474 | 500 | 524 | 548 | 573 |
| 192 | 584 | 626 | 666 | 707 | 748 |
| 194 | 722 | 768 | 816 | 866 | 922 |
| 196 | 845 | 919 | 974 | 1020 | 1078 |
| 198 | 990 | 1041 | 1090 | 1139 | 1190 |
| 200 | 1197 | 1244 | 1284 | 1324 | 1366 |
| 202 | 1230 | 1283 | 1328 | 1374 | 1422 |
| 204 | 1244 | 1302 | 1350 | 1400 | 1452 |
| 206 | 1239 | 1299 | 1350 | 1402 | 1457 |
| 208 | 1216 | 1277 | 1328 | 1381 | 1435 |
| 210 | 1177 | 1237 | 1286 | 1337 | 1391 |
| 212 | 1124 | 1180 | 1227 | 1276 | 1326 |
| 214 | 1060 | 1111 | 1154 | 1198 | 1245 |
| 216 | 986 | 1032 | 1070 | 1110 | 1151 |
| 218 | 907 | 947 | 980 | 1014 | 1049 |
| 220 | 824 | 858 | 885 | 914 | 943 |
| 222 | 741 | 768 | 790 | 813 | 836 |
| 224 | 659 | 680 | 697 | 714 | 732 |
| 226 | 580 | 595 | 608 | 620 | 633 |
| 228 | 505 | 516 | 524 | 533 | 541 |
| 230 | 436 | 442 | 447 | 452 | 457 |
| 232 | 373 | 376 | 378 | 380 | 382 |
| 234 | 316 | 316 | 316 | 316 | 316 |
| 236 | 266 | 264 | 262 | 260 | 259 |
| 238 | 222 | 218 | 215 | 212 | 210 |

TABLE 4a (Cont.)

| λ (nm) | 295K | 270K | 250K | 230K | 210K |
|----------------|--------|--------|---------|---------|---------|
| 240 | 183 | 179 | 175 | 172 | 168 |
| 242 | 150 | 145 | 141 | 138 | 134 |
| 244 | 123 | 117 | 113 | 109 | 106 |
| 246 | 99.2 | 92.0 | 90.0 | 86.1 | 82.5 |
| 248 | 79.7 | 74.7 | 70.9 | 67.3 | 63.9 |
| 250 | 63.7 | 59.0 | 55.5 | 52.2 | 49.1 |
| 252 | 50.5 | 46.2 | 43.1 | 40.2 | 37.5 |
| 254 | 39.8 | 36.0 | 33.3 | 30.7 | 28.3 |
| 256 | 31.2 | 27.9 | 25.5 | 23.3 | 21.3 |
| 258 | 24.3 | 21.4 | 19.4 | 17.5 | 15.9 |
| 260 | 18.8 | 16.4 | 14.7 | 13.1 | 11.7 |
| 262 | 14.5 | 12.4 | 11.0 | 9.73 | 8.61 |
| 264 | 11.1 | 9.39 | 8.21 | 7.18 | 6.28 |
| 266 | 8.46 | 7.05 | 6.09 | 5.26 | 4.54 |
| 268 | 6.42 | 5.26 | 4.49 | 3.83 | 3.26 |
| 270 | 4.84 | 3.90 | 3.29 | 2.77 | 2.33 |
| 272 | 3.63 | 2.88 | 2.39 | 1.99 | 1.65 |
| 274 | 2.71 | 2.11 | 1.73 | 1.42 | 1.16 |
| 276 | 2.01 | 1.54 | 1.24 | 1.00 | 0.810 |
| 278 | 1.48 | 1.11 | 0.887 | 0.706 | 0.562 |
| 280 | 1.09 | 0.803 | 0.629 | 0.493 | 0.386 |
| 282 | 0.796 | 0.576 | 0.444 | 0.342 | 0.264 |
| 284 | 0.579 | 0.410 | 0.311 | 0.236 | 0.179 |
| 286 | 0.419 | 0.290 | 0.216 | 0.161 | 0.120 |
| 288 | 0.301 | 0.204 | 0.149 | 0.109 | 0.0802 |
| 290 | 0.215 | 0.143 | 0.103 | 0.0737 | 0.0530 |
| 292 | 0.153 | 0.0990 | 0.0698 | 0.0493 | 0.0348 |
| 294 | 0.108 | 0.0683 | 0.0472 | 0.0327 | 0.0226 |
| 296 | 0.0761 | 0.0468 | 0.0317 | 0.0215 | 0.0146 |
| 298 | 0.0532 | 0.0318 | 0.0211 | 0.0140 | 0.00929 |
| 300 | 0.0369 | 0.0215 | 0.0139 | 0.00905 | 0.00587 |
| 302 | 0.0255 | 0.0144 | 0.00914 | 0.00579 | 0.00367 |

TABLE 4b : Absorption cross-sections of CF_2BrCl averaged over the spectral intervals used in atmospheric modelling calculations for five selected temperatures (295, 270, 250, 230, and 210K)

(wavenumber intervals : 500 cm^{-1})

$\sigma(\lambda) \times 10^{21} (\text{cm}^2 \text{ molec.}^{-1})$

| N° | $\lambda(\text{nm})$ | 295K | 270K | 250K | 230K | 210K |
|----|----------------------|------|------|------|------|------|
| 43 | 169.5-172.4 | 2770 | 2738 | 2710 | 2686 | 2661 |
| 44 | 172.4-173.9 | 1999 | 1960 | 1920 | 1880 | 1841 |
| 45 | 173.9-175.4 | 1575 | 1535 | 1498 | 1478 | 1449 |
| 46 | 175.4-177.0 | 1165 | 1147 | 1131 | 1115 | 1100 |
| 47 | 177.0-178.6 | 878 | 866 | 855 | 845 | 837 |
| 48 | 178.6-180.2 | 643 | 642 | 641 | 641 | 641 |
| 49 | 180.2-181.8 | 487 | 487 | 487 | 487 | 487 |
| 50 | 181.8-183.5 | 388 | 390 | 391 | 391 | 392 |
| 51 | 183.5-185.2 | 341 | 347 | 352 | 357 | 361 |
| 52 | 185.2-186.9 | 342 | 350 | 356 | 362 | 367 |
| 53 | 186.9-188.7 | 384 | 399 | 415 | 430 | 444 |
| 54 | 188.7-190.5 | 448 | 472 | 492 | 515 | 538 |
| 55 | 190.5-192.3 | 550 | 587 | 620 | 653 | 703 |
| 56 | 192.3-194.2 | 665 | 717 | 760 | 805 | 852 |
| 57 | 194.2-196.1 | 799 | 840 | 893 | 947 | 1000 |
| 58 | 196.1-198.0 | 917 | 970 | 1030 | 1090 | 1150 |
| 59 | 198.0-200.0 | 1080 | 1131 | 1177 | 1223 | 1269 |
| 60 | 200.0-202.0 | 1196 | 1266 | 1309 | 1352 | 1397 |
| 61 | 202.0-204.1 | 1239 | 1296 | 1343 | 1391 | 1441 |
| 62 | 204.1-206.2 | 1243 | 1303 | 1353 | 1404 | 1458 |
| 63 | 206.2-208.3 | 1227 | 1288 | 1339 | 1391 | 1446 |
| 64 | 208.3-210.5 | 1191 | 1251 | 1300 | 1352 | 1406 |
| 65 | 210.5-212.8 | 1135 | 1191 | 1238 | 1288 | 1339 |
| 66 | 212.8-215.0 | 1063 | 1115 | 1158 | 1203 | 1249 |
| 67 | 215.0-217.4 | 979 | 1024 | 1062 | 1101 | 1141 |
| 68 | 217.4-219.8 | 882 | 920 | 951 | 984 | 1017 |
| 69 | 219.8-222.2 | 783 | 813 | 837 | 863 | 889 |
| 70 | 222.2-224.7 | 681 | 704 | 722 | 741 | 760 |
| 71 | 224.7-227.3 | 580 | 595 | 608 | 620 | 633 |
| 72 | 227.3-229.9 | 484 | 493 | 500 | 508 | 515 |
| 73 | 229.9-232.6 | 396 | 400 | 403 | 406 | 409 |
| 74 | 232.6-235.3 | 318 | 318 | 318 | 318 | 318 |
| 75 | 235.3-238.1 | 250 | 247 | 245 | 243 | 241 |
| 76 | 238.1-241.0 | 192 | 188 | 185 | 181 | 178 |
| 77 | 241.0-243.9 | 144 | 139 | 135 | 131 | 127 |

TABLE 4b (cont.)

| N° | λ (nm) | 295K | 270K | 250K | 230K | 210K |
|----|----------------|--------|--------|--------|---------|---------|
| 78 | 243.9-246.9 | 106 | 101 | 96.5 | 92.6 | 88.9 |
| 79 | 246.9-250.0 | 75.4 | 70.5 | 66.8 | 63.2 | 59.9 |
| 80 | 250.0-253.2 | 53.5 | 49.2 | 46.0 | 42.9 | 40.1 |
| 81 | 253.2-256.4 | 36.1 | 32.5 | 29.9 | 27.5 | 25.3 |
| 82 | 256.4-259.7 | 24.3 | 21.4 | 19.4 | 17.5 | 15.9 |
| 83 | 259.7-263.2 | 15.5 | 13.3 | 11.8 | 10.5 | 9.31 |
| 84 | 263.2-266.7 | 9.70 | 8.14 | 7.08 | 6.15 | 5.35 |
| 85 | 266.7-270.3 | 5.98 | 4.88 | 4.15 | 3.53 | 3.00 |
| 86 | 270.3-274.0 | 3.58 | 2.83 | 2.35 | 1.95 | 1.62 |
| 87 | 274.0-277.8 | 2.04 | 1.56 | 1.26 | 1.02 | 0.825 |
| 88 | 277.8-281.7 | 1.12 | 0.830 | 0.652 | 0.511 | 0.401 |
| 89 | 281.7-285.7 | 0.608 | 0.431 | 0.328 | 0.249 | 0.190 |
| 90 | 285.7-289.9 | 0.311 | 0.211 | 0.155 | 0.114 | 0.0835 |
| 91 | 289.9-294.1 | 0.153 | 0.0990 | 0.0698 | 0.0493 | 0.0348 |
| 92 | 294.1-298.5 | 0.0721 | 0.0442 | 0.0298 | 0.0202 | 0.0136 |
| 93 | 298.5-303.0 | 0.0318 | 0.0183 | 0.0118 | 0.00758 | 0.00487 |

TABLE 5 : Parameters A_i and B_i for polynomial expression of $\sigma(\lambda, T)$ of bromo-fluoro-methanes

CF_3Br

| | | |
|-------------------------------|---|--------------------------------|
| $A_0 = 62.563$ | : | $B_0 = -9.1755 \cdot 10^{-1}$ |
| $A_1 = -2.0068$ | : | $B_1 = 1.8575 \cdot 10^{-2}$ |
| $A_2 = 1.6592 \cdot 10^{-2}$ | : | $B_2 = -1.3857 \cdot 10^{-4}$ |
| $A_3 = -5.6465 \cdot 10^{-5}$ | : | $B_3 = 4.5066 \cdot 10^{-7}$ |
| $A_4 = 6.7459 \cdot 10^{-8}$ | : | $B_4 = -5.3803 \cdot 10^{-10}$ |

T range : 210 - 300 K

λ range : 178 - 280 nm

CF_2Br_2

| | | |
|-------------------------------|---|-------------------------------|
| $A_0 = -206.28$ | : | $B_0 = 1.0460 \cdot 10^{-1}$ |
| $A_1 = 2.3726$ | : | $B_1 = -1.4124 \cdot 10^{-3}$ |
| $A_2 = -1.0527 \cdot 10^{-2}$ | : | $B_2 = 6.9015 \cdot 10^{-6}$ |
| $A_3 = 1.9239 \cdot 10^{-5}$ | : | $B_3 = -1.5164 \cdot 10^{-8}$ |
| $A_4 = -1.2242 \cdot 10^{-8}$ | : | $B_4 = 1.3990 \cdot 10^{-11}$ |

T range : 210 - 300 K

λ range : 222 - 304 nm

CF_2BrCl

| | | |
|-------------------------------|---|-------------------------------|
| $A_0 = -134.80$ | : | $B_0 = 3.3070 \cdot 10^{-1}$ |
| $A_1 = 1.7084$ | : | $B_1 = -5.0957 \cdot 10^{-3}$ |
| $A_2 = -9.1540 \cdot 10^{-3}$ | : | $B_2 = 2.9361 \cdot 10^{-5}$ |
| $A_3 = 2.1644 \cdot 10^{-5}$ | : | $B_3 = -7.6198 \cdot 10^{-8}$ |
| $A_4 = -1.9863 \cdot 10^{-8}$ | : | $B_4 = 7.6825 \cdot 10^{-11}$ |

T range : 210 - 300 K

λ range : 200 - 302 nm

TABLE 6 : Photodissociation coefficients versus altitude in the stratosphere

CF_3Br

λ range : 175-290nm

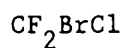
| Z(km) | sec χ = 1 | | | sec χ = 2 | | |
|----------|---|---------------------------------------|------------------|---|---------------------------------------|------------------|
| | $J(\text{s}^{-1})$ $\sigma(295\text{K})^a$ | $J(\text{s}^{-1})$ $\sigma = f(T)$ | J_{rel} | $J(\text{s}^{-1})$ $\sigma(295\text{K})^a$ | $J(\text{s}^{-1})$ $\sigma = f(T)$ | J_{rel} |
| 15 | $3.591 \cdot 10^{-9}$ | $4.115 \cdot 10^{-9}$ | 1.146 | $7.714 \cdot 10^{-12}$ | $8.957 \cdot 10^{-12}$ | 1.161 |
| 20 | $3.878 \cdot 10^{-8}$ | $4.447 \cdot 10^{-8}$ | 1.147 | $6.901 \cdot 10^{-10}$ | $8.004 \cdot 10^{-10}$ | 1.160 |
| 25 | $2.075 \cdot 10^{-7}$ | $2.351 \cdot 10^{-7}$ | 1.133 | $1.486 \cdot 10^{-8}$ | $1.704 \cdot 10^{-8}$ | 1.147 |
| 30 | $7.468 \cdot 10^{-7}$ | $8.296 \cdot 10^{-7}$ | 1.111 | $1.425 \cdot 10^{-7}$ | $1.609 \cdot 10^{-7}$ | 1.129 |
| 35 | $2.067 \cdot 10^{-6}$ | $2.213 \cdot 10^{-6}$ | 1.071 | $7.593 \cdot 10^{-7}$ | $8.302 \cdot 10^{-7}$ | 1.093 |
| 40 | $4.673 \cdot 10^{-6}$ | $4.776 \cdot 10^{-6}$ | 1.022 | $2.674 \cdot 10^{-6}$ | $2.789 \cdot 10^{-6}$ | 1.043 |
| 45 | $7.552 \cdot 10^{-6}$ | $7.493 \cdot 10^{-6}$ | .992 | $5.758 \cdot 10^{-6}$ | $5.781 \cdot 10^{-6}$ | 1.004 |
| 50 | $9.260 \cdot 10^{-6}$ | $9.109 \cdot 10^{-6}$ | .984 | $8.266 \cdot 10^{-6}$ | $8.168 \cdot 10^{-6}$ | .988 |
| ∞ | $1.049 \cdot 10^{-5}$ | | | | | |

CF_2Br_2

λ range : 170-307nm

| Z(km) | sec χ = 1 | | | sec χ = 2 | | |
|----------|---|---------------------------------------|------------------|---|---------------------------------------|------------------|
| | $J(\text{s}^{-1})$ $\sigma(295\text{K})^a$ | $J(\text{s}^{-1})$ $\sigma = f(T)$ | J_{rel} | $J(\text{s}^{-1})$ $\sigma(295\text{K})^a$ | $J(\text{s}^{-1})$ $\sigma = f(T)$ | J_{rel} |
| 15 | $5.571 \cdot 10^{-8}$ | $4.250 \cdot 10^{-8}$ | .763 | $5.091 \cdot 10^{-9}$ | $1.569 \cdot 10^{-9}$ | .308 |
| 20 | $3.538 \cdot 10^{-7}$ | $3.844 \cdot 10^{-7}$ | 1.087 | $1.310 \cdot 10^{-8}$ | $8.280 \cdot 10^{-9}$ | .632 |
| 25 | $1.874 \cdot 10^{-6}$ | $2.123 \cdot 10^{-6}$ | 1.133 | $1.287 \cdot 10^{-7}$ | $1.348 \cdot 10^{-7}$ | 1.047 |
| 30 | $7.700 \cdot 10^{-6}$ | $8.725 \cdot 10^{-6}$ | 1.133 | $1.218 \cdot 10^{-6}$ | $1.366 \cdot 10^{-6}$ | 1.121 |
| 35 | $2.803 \cdot 10^{-5}$ | $3.112 \cdot 10^{-5}$ | 1.110 | $7.864 \cdot 10^{-6}$ | $8.747 \cdot 10^{-6}$ | 1.112 |
| 40 | $9.850 \cdot 10^{-5}$ | $1.054 \cdot 10^{-4}$ | 1.070 | $4.179 \cdot 10^{-5}$ | $4.511 \cdot 10^{-5}$ | 1.079 |
| 45 | $2.449 \cdot 10^{-4}$ | $2.523 \cdot 10^{-4}$ | 1.030 | $1.482 \cdot 10^{-4}$ | $1.541 \cdot 10^{-4}$ | 1.040 |
| 50 | $3.735 \cdot 10^{-4}$ | $3.794 \cdot 10^{-4}$ | 1.016 | $3.013 \cdot 10^{-4}$ | $3.072 \cdot 10^{-4}$ | 1.020 |
| ∞ | $4.727 \cdot 10^{-4}$ | | | | | |

TABLE 6 : (cont).

 λ range : 170-307nm

| Z(km) | sec χ = 1 | | | sec χ = 2 | | |
|----------|---|--|------------------|---|--|------------------|
| | J(s ⁻¹) $\sigma(295K)^a$ | J(s ⁻¹) $\sigma = f(T)$ | J _{rel} | J(s ⁻¹) $\sigma(295K)^a$ | J(s ⁻¹) $\sigma = f(T)$ | J _{rel} |
| 15 | 3.598 10 ⁻⁸ | 4.062 10 ⁻⁸ | 1.129 | 1.544 10 ⁻¹⁰ | 1.013 10 ⁻¹⁰ | .656 |
| 20 | 3.781 10 ⁻⁷ | 4.372 10 ⁻⁷ | 1.156 | 6.884 10 ⁻⁹ | 7.813 10 ⁻⁹ | 1.135 |
| 25 | 2.016 10 ⁻⁶ | 2.316 10 ⁻⁶ | 1.149 | 1.451 10 ⁻⁷ | 1.662 10 ⁻⁷ | 1.146 |
| 30 | 7.243 10 ⁻⁶ | 8.243 10 ⁻⁶ | 1.138 | 1.384 10 ⁻⁶ | 1.575 10 ⁻⁶ | 1.138 |
| 35 | 2.021 10 ⁻⁵ | 2.250 10 ⁻⁵ | 1.113 | 7.366 10 ⁻⁶ | 8.225 10 ⁻⁶ | 1.117 |
| 40 | 4.745 10 ⁻⁵ | 5.102 10 ⁻⁵ | 1.075 | 2.639 10 ⁻⁵ | 2.856 10 ⁻⁵ | 1.082 |
| 45 | 8.263 10 ⁻⁵ | 8.573 10 ⁻⁵ | 1.038 | 6.023 10 ⁻⁵ | 6.296 10 ⁻⁵ | 1.045 |
| 50 | 1.070 10 ⁻⁴ | 1.094 10 ⁻⁴ | 1.023 | 9.301 10 ⁻⁵ | 9.544 10 ⁻⁵ | 1.026 |
| ∞ | 1.263 10 ⁻⁴ | | | | | |

^a Temperature independent cross-section.J_{rel} relative value J(T)/J(295K).

TABLE 7 : Photodissociation coefficients versus altitude in the troposphere.

CF_3Br

λ range : 175-335nm

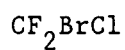
| Z(km) | sec χ = 1 | | | sec χ = 2 | | |
|----------|---|---------------------------------------|------------------|---|---------------------------------------|------------------|
| | $J(\text{s}^{-1})$ $\sigma(295\text{K})^a$ | $J(\text{s}^{-1})$ $\sigma = f(T)$ | J_{rel} | $J(\text{s}^{-1})$ $\sigma(295\text{K})^a$ | $J(\text{s}^{-1})$ $\sigma = f(T)$ | J_{rel} |
| 0 | $5.575 \cdot 10^{-11}$ | $4.670 \cdot 10^{-11}$ | .838 | $3.001 \cdot 10^{-11}$ | $2.498 \cdot 10^{-11}$ | .832 |
| 2 | $5.640 \cdot 10^{-11}$ | $3.272 \cdot 10^{-11}$ | .580 | $3.037 \cdot 10^{-11}$ | $1.721 \cdot 10^{-11}$ | .567 |
| 4 | $5.705 \cdot 10^{-11}$ | $1.813 \cdot 10^{-11}$ | .318 | $3.074 \cdot 10^{-11}$ | $9.192 \cdot 10^{-12}$ | .299 |
| 6 | $5.790 \cdot 10^{-11}$ | $1.267 \cdot 10^{-11}$ | .217 | $3.114 \cdot 10^{-11}$ | $6.221 \cdot 10^{-12}$ | .200 |
| 8 | $6.240 \cdot 10^{-11}$ | $1.065 \cdot 10^{-11}$ | .171 | $3.168 \cdot 10^{-11}$ | $3.185 \cdot 10^{-12}$ | .101 |
| 10 | $1.110 \cdot 10^{-10}$ | $6.012 \cdot 10^{-11}$ | .542 | $3.241 \cdot 10^{-11}$ | $1.104 \cdot 10^{-12}$ | .034 |
| 12 | $4.621 \cdot 10^{-10}$ | $4.613 \cdot 10^{-10}$ | .998 | $3.339 \cdot 10^{-11}$ | $1.148 \cdot 10^{-12}$ | .034 |
| 14 | $1.974 \cdot 10^{-9}$ | $2.193 \cdot 10^{-9}$ | 1.111 | $3.649 \cdot 10^{-11}$ | $3.686 \cdot 10^{-12}$ | .101 |
| ∞ | $1.049 \cdot 10^{-5}$ | | | | | |

CF_2Br_2

λ range : 170-335nm

| Z(km) | sec χ = 1 | | | sec χ = 2 | | |
|----------|---|---------------------------------------|------------------|---|---------------------------------------|------------------|
| | $J(\text{s}^{-1})$ $\sigma(295\text{K})^a$ | $J(\text{s}^{-1})$ $\sigma = f(T)$ | J_{rel} | $J(\text{s}^{-1})$ $\sigma(295\text{K})^a$ | $J(\text{s}^{-1})$ $\sigma = f(T)$ | J_{rel} |
| 0 | $7.365 \cdot 10^{-8}$ | $6.450 \cdot 10^{-8}$ | .876 | $4.061 \cdot 10^{-8}$ | $3.512 \cdot 10^{-8}$ | .865 |
| 2 | $7.448 \cdot 10^{-8}$ | $5.111 \cdot 10^{-8}$ | .686 | $4.107 \cdot 10^{-8}$ | $2.719 \cdot 10^{-8}$ | .662 |
| 4 | $7.533 \cdot 10^{-8}$ | $4.064 \cdot 10^{-8}$ | .539 | $4.154 \cdot 10^{-8}$ | $2.111 \cdot 10^{-8}$ | .508 |
| 6 | $7.626 \cdot 10^{-8}$ | $3.244 \cdot 10^{-8}$ | .425 | $4.204 \cdot 10^{-8}$ | $1.645 \cdot 10^{-8}$ | .391 |
| 8 | $7.756 \cdot 10^{-8}$ | $2.613 \cdot 10^{-8}$ | .337 | $4.274 \cdot 10^{-8}$ | $1.292 \cdot 10^{-8}$ | .302 |
| 10 | $7.964 \cdot 10^{-8}$ | $2.168 \cdot 10^{-8}$ | .272 | $4.367 \cdot 10^{-8}$ | $1.024 \cdot 10^{-8}$ | .235 |
| 12 | $8.451 \cdot 10^{-8}$ | $2.347 \cdot 10^{-8}$ | .278 | $4.478 \cdot 10^{-8}$ | $9.384 \cdot 10^{-9}$ | .210 |
| 14 | $9.884 \cdot 10^{-8}$ | $3.849 \cdot 10^{-8}$ | .389 | $4.601 \cdot 10^{-8}$ | $9.718 \cdot 10^{-9}$ | .211 |
| ∞ | $4.728 \cdot 10^{-4}$ | | | | | |

TABLE 7 : (cont.)

 λ range : 170-335nm

| Z(km) | sec χ = 1 | | | sec χ = 2 | | |
|----------|---|--|------------------|---|--|------------------|
| | J(s ⁻¹) $\sigma(295K)^a$ | J(s ⁻¹) $\sigma = f(T)$ | J _{rel} | J(s ⁻¹) $\sigma(295K)^a$ | J(s ⁻¹) $\sigma = f(T)$ | J _{rel} |
| 0 | 4.168 10 ⁻⁹ | 3.430 10 ⁻⁹ | .823 | 1.680 10 ⁻⁹ | 1.354 10 ⁻⁹ | .806 |
| 2 | 4.238 10 ⁻⁹ | 2.439 10 ⁻⁹ | .576 | 1.709 10 ⁻⁹ | 9.267 10 ⁻¹⁰ | .542 |
| 4 | 4.311 10 ⁻⁹ | 1.744 10 ⁻⁹ | .405 | 1.740 10 ⁻⁹ | 6.380 10 ⁻¹⁰ | .367 |
| 6 | 4.389 10 ⁻⁹ | 1.255 10 ⁻⁹ | .286 | 1.773 10 ⁻⁹ | 4.419 10 ⁻¹⁰ | .249 |
| 8 | 4.534 10 ⁻⁹ | 9.546 10 ⁻¹⁰ | .211 | 1.819 10 ⁻⁹ | 3.100 10 ⁻¹⁰ | .170 |
| 10 | 5.139 10 ⁻⁹ | 1.243 10 ⁻⁹ | .242 | 1.881 10 ⁻⁹ | 2.207 10 ⁻¹⁰ | .117 |
| 12 | 8.702 10 ⁻⁹ | 5.112 10 ⁻⁸ | .587 | 1.957 10 ⁻⁹ | 1.957 10 ⁻¹⁰ | .100 |
| 14 | 2.352 10 ⁻⁸ | 2.213 10 ⁻⁸ | .941 | 2.061 10 ⁻⁹ | 2.303 10 ⁻¹⁰ | .112 |
| ∞ | 1.263 10 ⁻⁴ | | | | | |

^a Temperature independent cross-section.

J_{rel} relative value J(T)/J(295K).